AD-A187 100 PLASMA THEORY AND SIMULATION(U) CALIFORNIA UNIV 1/1
BERKELEY ELECTRONICS RESEARCH LAB C K BIRDSALL
31 DEC 86 N00014-85-K-0809

UNCLASSIFIED F/G 20/9 NL

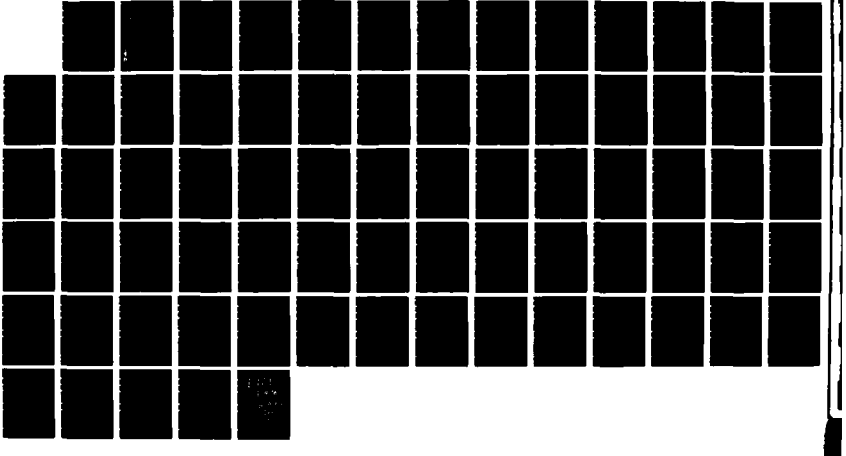

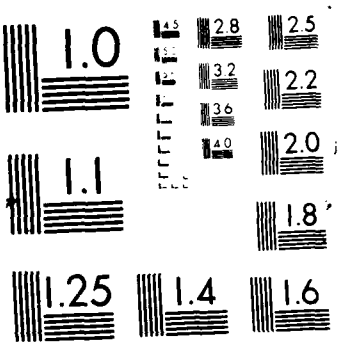
1.0
1.1
1.25
1.4
1.6
2.8
3.2
3.6
4.0
2.5
2.2
2.0
1.8

THIRD & FOURTH QUARTER PROGRESS REPORT 1986 ON PLASMA THEORY AND SIMULATION

July 1 to December 31, 1986

DOE Contract DE-FG03-86ER53220
ONR Contract N00014-85-K-0809
Varian Gift and MICRO
Hughes Aircraft Co. Gift

ELECTRONICS RESEARCH LABORATORY
College of Engineering
University of California, Berkeley, CA 94720

SECURITY CLASSIFICATION OF THI

REPORT DOC

READ INSTRUCTIONS
:FORE COMPLETING FORM

1. REPORT NUMBER

AD-A187 100

IENT'S CATALOG NUMBER

4. TITLE (and Subtitle)

Quarterly Progress Report, III, IV
July 1, 1986 - Dec. 31, 1986

OF REPORT & PERIOD COVERED

Progress, 7/1-12/31, 1986

6 PERFORMING ORG. REPORT NUMBER

7. AUTHOR(s)

Professor Charles K. Birdsall

8. CONTRACT OR GRANT NUMBER(s)

ONR N00014-85-K-0809

9. PERFORMING ORGANIZATION NAME AND ADDRESS

Electronics Research Laboratory
University of California
Berkeley, CA 94720

10 PROGRAM ELEMENT, PROJECT, TASK AREA & WORK UNIT NUMBERS

Element No. 61153N, Project Task Area RR01-09-01, Work Unit No. NR 012-742

11. CONTROLLING OFFICE NAME AND ADDRESS

ONR Physics Division
Department of the Navy, ONR
Arlington, VA 22217

12. REPORT DATE

13 NUMBER OF PAGES

14 MONITORING AGENCY NAME & ADDRESS(if different from Controlling Office)

15 SECURITY CLASS. (of this report)

Unclassified

15a DECLASSIFICATION/ DOWNGRADING SCHEDULE

16. DISTRIBUTION STATEMENT (of this Report)

Approved for public release; distribution unlimited

17. DISTRIBUTION STATEMENT (of the abstract entered in Block 20, if different from Report)

18. SUPPLEMENTARY NOTES

Our group uses theory and simulation as tools in order to increase the understanding of plasma instabilities, heating, transport, plasma-wall interactions, and large potentials in plasmas. We also work on the improvement of simulation both theoretically and practically.

19. KEY WORDS (Continue on reverse side if necessary and identify by block number)

Research in plasma theory and simulation, plasma-wall interactions, large potentials in plasmas.

20. ABSTRACT (Continue on reverse side if necessary and identify by block number)

See reverse side

DD FORM 1 JAN 73 1473 EDITION OF 1 NOV 65 IS OBSOLETE

S/N 0102-LF-014-6601

Unclassified

SECURITY CLASSIFICATION OF THIS PAGE (When Data Entered)

20. ABSTRACT

General Plasma Theory and Simulation

A. The Pierce diode linear behavior with external R, C, or L was verified very accurately by particle simulation. Final report issued.

B. The Pierce diode non-linear equilibria with R, C, or L are described theoretically and explored via computer simulation. Final report issued.

C. A simple model of the sheath outside the separatrix of an FRC was modeled electrostatically in 2d and large potentials due to the magnetic well and peak were found; these may explain the anomolously high ion confinement in the FRC edge layer. Memorandum to be issued.

D. A planar plasma source with cold ions and warm electrons produces a source sheath with sufficient potential drop to accelerate ions to sound velocity, which obviates the need for a Bohm pre-collector-sheath electric field.

Plasma-Wall Physics, Theory and Simulation

A. Collector Sheath, Presheath, and Source Sheath in a Collisionless, Finite Ion Temperature Plasma; final report in preparation.

B. Potential Drop and Transport in a Bounded Plasma with Ion Relfection at the Collector; final report in preparation.

C. Potential Drop and Transport in a Bounded Plasma with Secondary Electron Emission at the Collector; final report in preparation.

*, ** D. A movie has been made displaying the long-lived vortices resulting from the Kelvin-Helmholtz instability in a magnetized sheath.

Code Development and Software Distribution

*** A. A relativistic Monte Carlo binary (Coulomb) collision model has been developed and tested for inclusion into the electrostatic particle simulation code TESS.

*** B. Two direct implicit time integration schemes are tested for self-heating and self-cooling and regions of neither are found as a function of Δt and Δx for the model of a freely expanding plasma slab.

Major support is from DOE.

* Supported in part by ONR.

** Supported in part by Varian/MICRO.

*** Supported in part by IR&D Grant from LLNL.

THIRD AND FOURTH QUARTER PROGRESS REPORT
ON
PLASMA THEORY AND SIMULATION

July 1 to December 31, 1986

Our research group uses both theory and simulation as tools in order to increase the understanding of instabilities, heating, transport, plasma-wall interactions, and large potentials in plasmas. We also work on the improvement of simulation, both theoretically and practically.

Our staff is:

Professor C. K. Birdsall *Principal Investigator*	191M	Cory Hall	(643-6631)
Dr. Kim Theilhaber *Post-doctorate*	187M	Cory Hall	(642-3477)
Mr. William Lawson	199MD	Cory Hall	(642-1297)
Mr. Scott Parker	199MD	Cory Hall	(642-1297)
Mr. Robert Pierce	199MD	Cory Hall	(642-1297)
Mr. Richard Procassini	199MD	Cory Hall	(642-1297)
Ms. Lou Ann Schwager *Research Assistants (students)*	199MD	Cory Hall	(642-1297)

Our Advisors and Associates are:

Dr. Ilan Roth *Physicist, Space Science Lab., UCB*	304	SSL, Campus	(642-1327)
Dr. Bruce Cohen	L630	LLNL, Livermore	(422-9823)
Dr. Alex Friedman	L630	LLNL	(422-0827)
Dr. A. Bruce Langdon	L472	LLNL	(422-5444)
Dr. William Nevins *Physicists, Lawrence Livermore Natl. Lab.*	L630	LLNL	(422-7032)

December 31, 1986

DOE Contract DE-FG03-86ER53220
ONR Contract N00014-85-K-0809
Varian and MICRO Gift
Hughes Aircraft Co., Gift

ELECTRONICS RESEARCH LABORATORY

University of California
Berkeley, California 94720

Table of Contents

Major Support is from DOE.

* Supported in part by ONR.

** Supported in part by Varian/Micro.

*** Supported in part by IR&D Grant from LLNL.

SECTION I: GENERAL PLASMA THEORY AND SIMULATION

A. The Pierce Diode with an External Circuit. I. Simulations in the Linear Regime

William S. Lawson

Abstract

The linear theory for the eigen frequencies of the extended Pierce diode for resistive, capacitive, and inductive external circuits is tested via computer simulation with the PDW1 code, and is verified to within the accuracy of the simulation (between 1% and .01% depending on the circumstances). The simulations were remarkably inexpensive in terms of computer time, and could have been performed on a personal computer.

This work is to be issued as an *ERL Memorandum*.

B. The Pierce Diode with an External Circuit. II. Non-Linear Equilibria

William S. Lawson

This work is to be issued as an ERL Memorandum. The abstract follows.

C. Electrostatic Potential Formation Due to a Large Dip in the Magnetic Field with Application to FRC Confinement

S. E. Parker

This work is to be issued as an ERL Memorandum. The introduction follows.

D Ion Acceleration in the Plasma Source Sheath

C. K. Birdsall

B. THE PIERCE DIODE WITH AN EXTERNAL CIRCUIT. II.

NON-LINEAR EQUILIBRIA

William S. Lawson
Plasma Theory and Simulation Group
Electronics Research Laboratory
University of California
Berkeley, CA 94720

ABSTRACT

The non-uniform equilibria of the classical (short circuit) Pierce diode and the extended (series RLC external circuit) Pierce diode are described theoretically and explored via computer simulation. It is found that most equilibria are correctly predicted by theory, but that the continuous set of equilibria of the classical Pierce diode at $\alpha=2\pi$ are not observed. The stability characteristics of the non-uniform equilibria are also worked out, and are consistent with the simultations.

C. **Electrostatic Potential Formation**

Due to a Large Dip in the Magnetic Field

with Application to FRC Confinement

S. E. Parker
Plasma Theory and Simulation Group
Electronics Research Laboratory
University of California
Berkeley, CA 94720

ABSTRACT

Electrostatic effects may explain the enhanced plasma confinement observed in the open field line region of field-reversed configurations. We are studying the formation of electrostatic potentials due to nonuniform magnetic fields. This type of phenomenon is being modeled using particle simulation. Our two dimensional (x,y) electrostatic particle code, ES2 has been used to study the formation of electrostatic potentials due to magnetic wells and peaks with an injected flux of well magnetized electrons and weakly magnetized ions. These results are being used to help interpret the electrostatic potential contours outside the separatrix of a FRC, which are really cylindrical, (r,z). These potentials may explain the anomalously high ion confinement in the FRC edge layer. Our work naturally follows from the qualitative description of electrostatic effects on FRC confinement given by L. C. Steinhauer.

D. Ion Acceleration in the Plasma Source Sheath

C.K. Birdsall

This note is a calculation of the potential drop for a planar plasma source, across the *source sheath*, into a uniform plasma region defined by $\underline{E}=0$ and or perhaps $\partial^2\Phi/\partial x^2 = 0$. The calculation complements that of Bohm (1949) who obtained the potential drop at the other end of a plasma, at a planar *collector sheath*. The result is a relation between the source ion flux and the source sheath potential drop and the accompanying ion acceleration. This planar source sheath ion acceleration mechanism (or that from a distributed source) can provide the pre-collector-sheath ion acceleration as found necessary by Bohm.

[The analysis is elementary and may be in early works, such as Tonks and Langmuir (1929) and Harrison and Thompson (1959). Our apologies to such authors.]

MODEL, POISSON EQUATION

The model has a planar source of both warm electrons and cold ions shown in Fig. 1. Our object is to obtain analytically a value for the steady state potential drop near the source plate for monotonic potential decay. The model assumes cold ions, injected at $x = 0$ from rest, all traversing the device, with a given flux density Γ_i, independent of x. The warm electron density is assumed to be governed by a Boltzmann factor. For convenience, the source is at zero potential, $\phi(0) = 0$

The analysis assumes time independence, and uses conservation of energy and ion flux to set up Poisson's equation. At this step, one obtains what appears to be a maximum ion flux into a neutral plasma, occuring at an ion velocity equal to sound velocity. For the next step, integrate Poisson once, and apply the boundary condition of zero field at the plasma ($x \rightarrow \infty$). These steps relate the ion flux and the source sheath potential drop. The steps are similar to these of Bohm (1949) or Chen (1973) in their well known calculations of the collector sheath potential drop.

The ions are assumed start from rest at $x = 0$. Their energies are given by

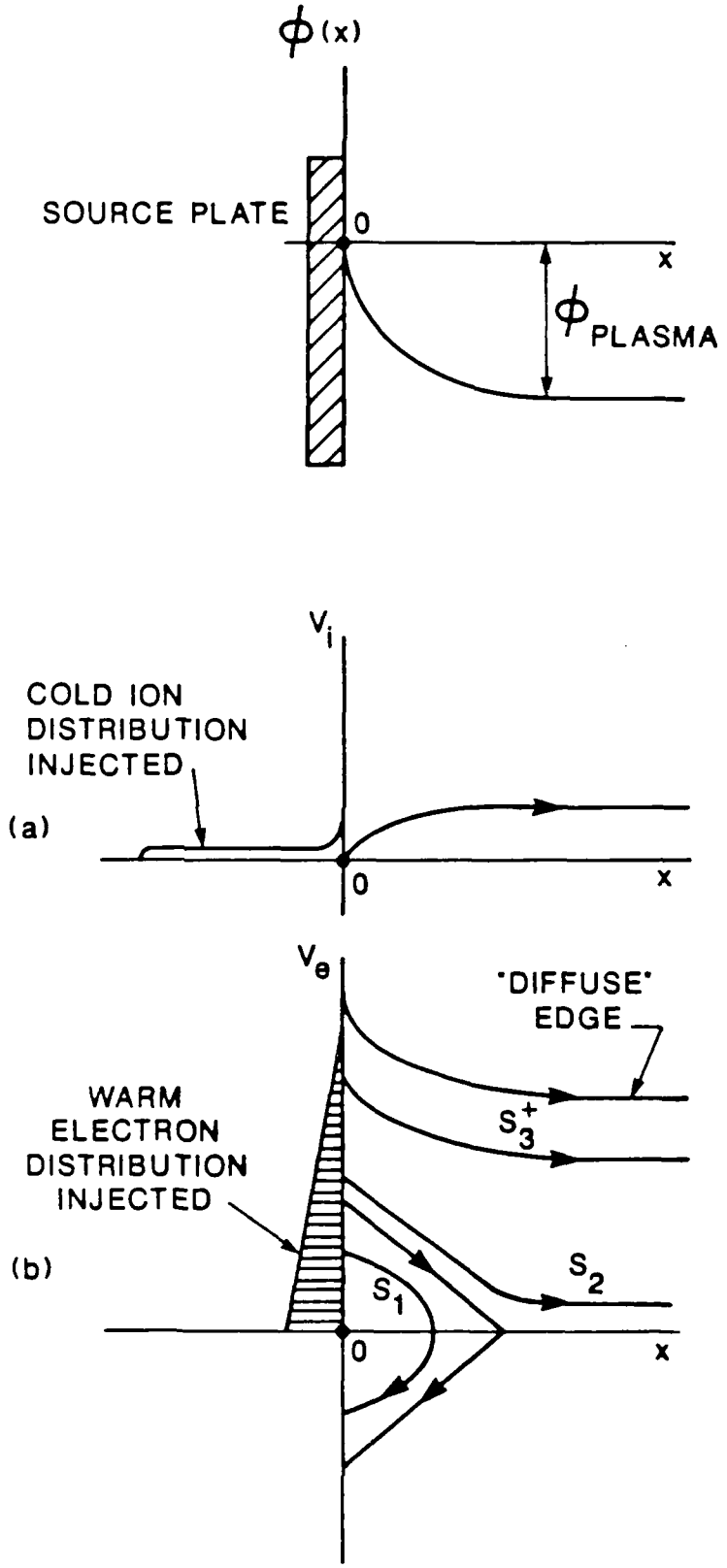

Figure 1. Model showing planar source (no volume generation of plasma), with assumed monotonic potential drop, along with (a) ion phase space (cold beam) and (b) electron phase space (warm injection).

$$\frac{1}{2} M u_i^2 = -e\,\Phi(x) > 0 \;,\; u_i = \sqrt{\frac{-2e}{M}\Phi(x)} \tag{1}$$

The ion flux density is given by

$$\Gamma_i = n_i(x)\, u_i(x) \tag{2}$$

which is constant with x. All ions are accelerated, starting from rest The ion density is

$$n_i = \frac{\Gamma_i}{u_i} = \frac{\Gamma_i}{\sqrt{\frac{-2e}{M}\Phi(x)}} \tag{3}$$

which blows up at the source, where the ion velocity vanishes. This implies a very copious source, similar to the infinite density, zero velocity source of Child's Law (1911).

The electron density is taken to be governed by a Boltzmann factor

$$n_e(x) = n_{eo}\, \exp\left[\, e\,\Phi(x)/kT_e \,\right] \tag{4}$$

n_{eo} is the electron density at the source plate, including both injected and returned electrons. This assumption is on shaky ground, as even at the source plate, where the distribution is a cut-off Gaussian.

Using these densities, Poisson's equation is

$$\frac{d^2\Phi(x)}{dx^2} = \frac{e}{\varepsilon_0}(n_e - n_i) = \frac{e}{\varepsilon_0}\left[n_{oe}\, \exp\left[\frac{e\,\Phi}{kT_e}\right] - \frac{\Gamma_i}{\sqrt{\frac{-2e}{M}\Phi}} \right] \tag{5}$$

For convenience, let

$$\eta \equiv \frac{-e\,\Phi}{kT_e} > 0 \;; \tag{6}$$

$$\xi \equiv \frac{x}{\lambda_D} = \left[\frac{n_{0e}e^2}{\varepsilon_0 kT_e}\right]^{1/2} x \;; \tag{7}$$

$$\frac{\Gamma_i}{\sqrt{-2e\frac{\Phi}{M}}} = \frac{\Gamma_i}{\sqrt{\frac{kT_e}{M}}\sqrt{2\eta}} = \frac{\Gamma_i}{v_{sound}\sqrt{2}}\frac{1}{\sqrt{\eta}} \equiv F\frac{n_{0e}}{\sqrt{\eta}} \tag{8}$$

where

$$F \equiv \frac{\Gamma_i}{n_{oe} v_s \sqrt{2}} \tag{9}$$

is the normalized ion flux.

Hence, Poisson's equation becomes, with $\eta = \eta(\xi)$

$$\eta'' = F\eta^{-\frac{1}{2}} - e^{-\eta} \tag{10}$$

INSIGHT INTO ION FLUX and ION VELOCITY

At this step, without employing any boundary conditions on the field at x = 0 or at $x = x_{plasma}$, we can find that value of potential η and flux F at which η'' changes sign, that is, $\eta''(\eta,F) = 0$ at

$$F(\eta'' = 0) = e^{-\eta}\sqrt{\eta} \tag{11}$$

This relation is plotted in Figure 2. The maximum value of flux is found at

$$\eta = 0.5 \tag{12}$$

$$F_{max} = \frac{1}{\sqrt{2e}} = 0.4288 \tag{13}$$

or

$$\Gamma_{i_{max}} = \frac{n_{oe} v_s}{\sqrt{e}} = 0.6065\ n_{oe} v_s \tag{14}$$

at

$$v_i = \sqrt{2\eta}\ v_s = v_s \tag{15}$$

These statements say that the maximum ion flux into a neutral plasma occurs with a potential drop from the source of $\eta = 0.5$ ($e\,\phi_{plasma} / kT_e = -0.5$) which accelerates the ions to sound velocity.

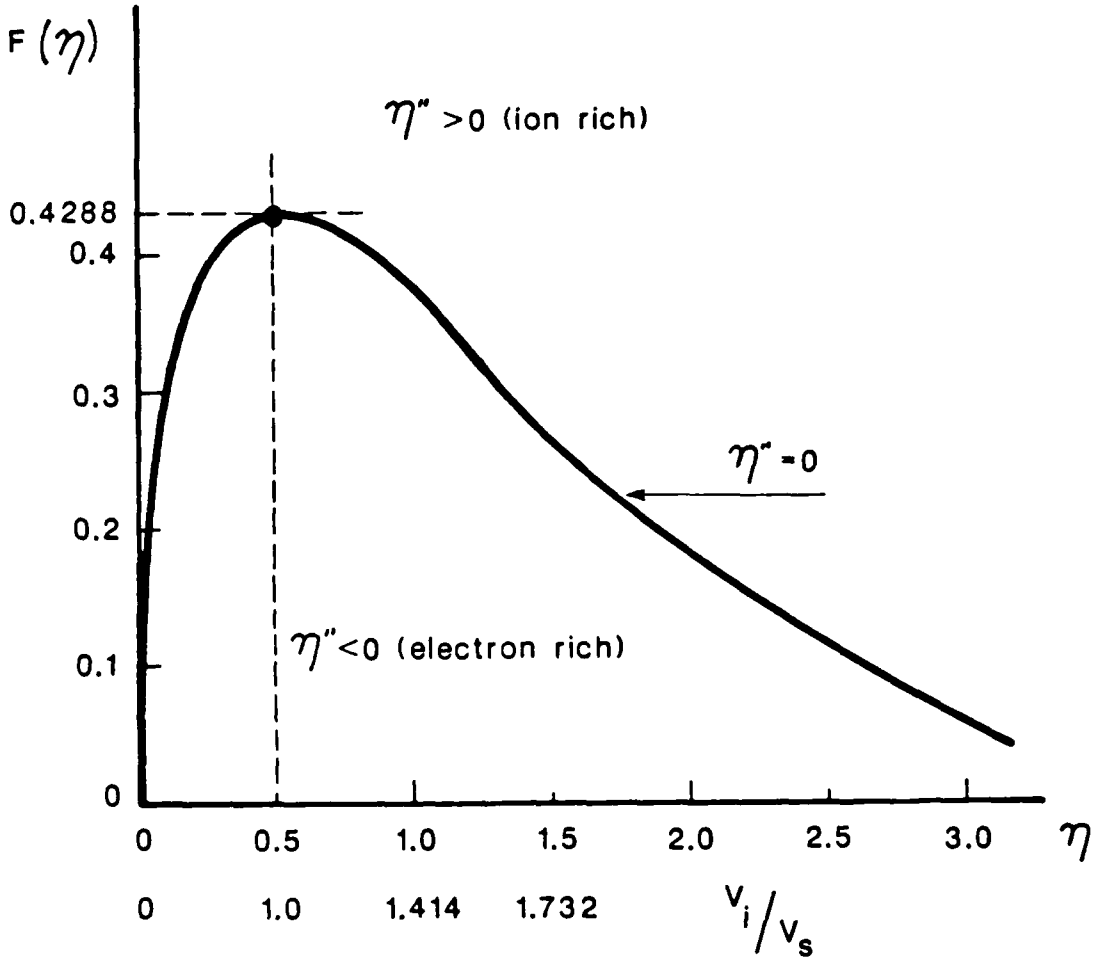

Figure 2. Locus of normalized ion flux density F as a function of potential $\eta(\xi)$, with ξ located at zero net charge density, $\eta''(\xi) = 0$. The ion velocity $v_i(\xi)/v_s = \sqrt{2\eta(\xi)}$ is also noted.

FIRST INTEGRATION; USE ZERO FIELD AT PLASMA

Integrate Equation (10) once by multiplying by η'; integrate $\int_0^{\xi} d\xi$,to obtain

$$\frac{1}{2}(\eta')^2 \Big|_0^{\xi} = 2F\,\eta^{1/2} \Big|_0^{\xi} + e^{-\eta} \Big|_0^{\xi} \tag{16}$$

The boundary conditions at the left side are : $\eta = 0$ at $\xi = 0$, $\eta'(0) = \eta'_0$. At the right side we take ξ to be in the plasma region where we postulate zero electric field, $\eta'(\xi) = 0$. Hence,

$$\frac{1}{2}(\eta'_0)^2 = 1 - \left[e^{-\eta} + 2F\eta^{1/2}\right] \tag{17}$$

We require the left hand side to be zero or positive, for real solutions; hence,

$$e^{-\eta} + 2F\sqrt{\eta} \le 1 \tag{18}$$

where η is measured at sheath edge, ξ, at the plasma potential, η_p.

This inequality may be rearranged in order to be read as a limitation on the ion flux, (for $\eta'(\xi) = 0$),

$$F \le (1 - e^{-\eta}) / (2\sqrt{\eta}) \equiv G(\eta) \tag{19}$$

For small η, $G(\eta) = \sqrt{\eta}/2$, for large η, $G(\eta) = 1/(2\sqrt{\eta})$; in between these values $G(\eta)$ has a maximum value of $G_{max} = 0.3191$ which occurs at $\eta \equiv \eta_c = 1.25643$

Taking $F < 0.3191 \equiv F_c$

$$\Gamma_i < 0.3191\sqrt{2}n_{oe}v_s = 0.4513\, n_{oe}v_s \equiv \Gamma_{ic} \tag{20}$$

When the ion flux $\Gamma_i < \Gamma_{ic}$ ($F < F_c$), then there are two values of η (η_1 and η_2 , see Figure 3) at which $F = G(\eta)$, meaning $\eta'(0)$. In between, $\eta_1 < \eta < \eta_2$, $F < G(\eta)$ so that $(\eta'^2_o) > 0$. Outside, $\eta < \eta_1$ and $\eta > \eta_2$, $F > G(\eta)$ so that $(\eta'^2_o) < 0$, taken as an indication of a solution that does not fit our assumptions (possibly time-dependent, possibly unstable, possibly multivalued v_i , or other).

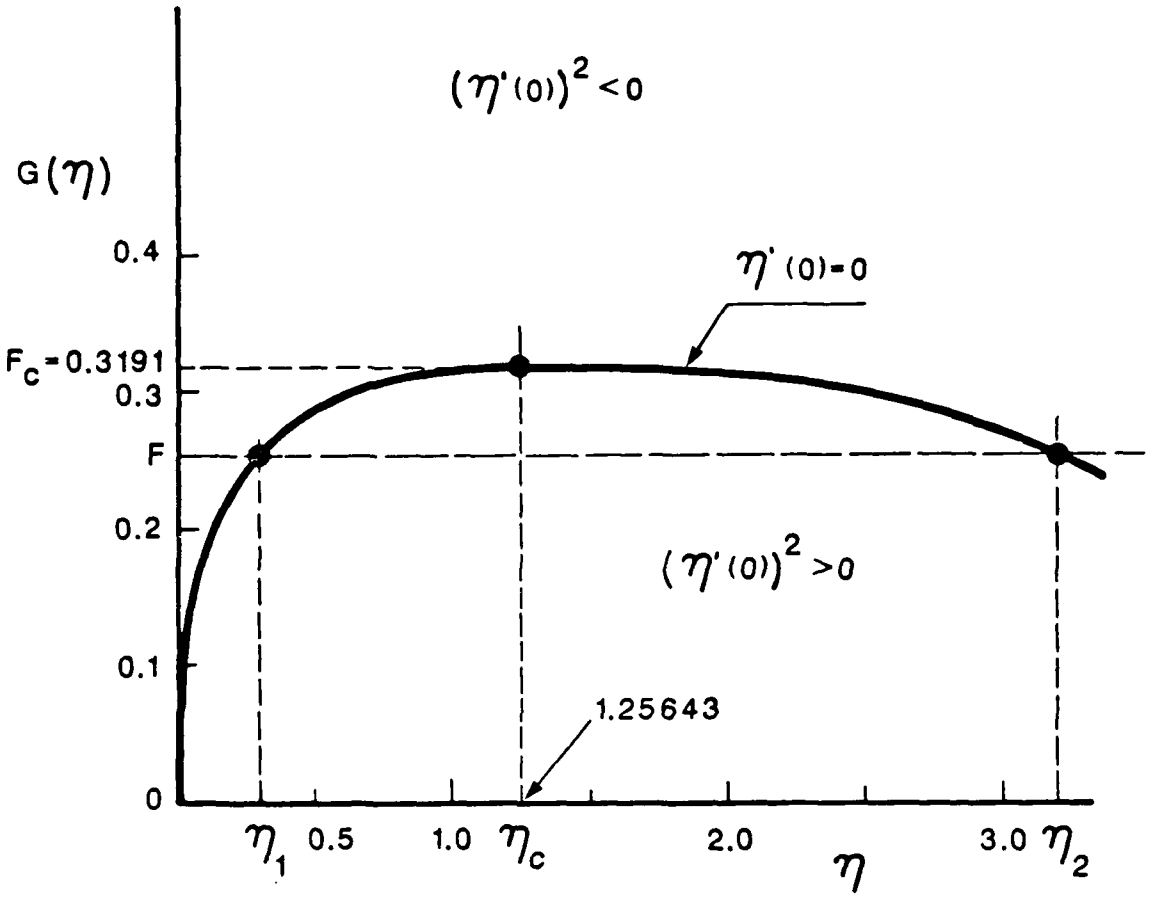

Figure 3. Flux function G(η) locating regions where the source field squared changes sign. There is a maximum ion flux value (F_c = 0.3191) of a critical potential (η_c = 1.25643).

For $\eta_1 < \eta_c$, with $F \leq G(\eta)$, $(\eta'(O))^2 \leq 0$, Equation (10) gives $\eta''_1(\xi) < 0$, all of which fits the expected $\eta(\xi)$ in Figure 1. However, for $\eta_2 > \eta_c$, $F = G(\eta)$ $\eta''_2(\xi) > 0$, which does not fit Figure 1.

As F is increased toward F_c, η_1 and η_2 coalesce to η_c, where $F = F_c$, $\eta = \eta_c$, $\eta'_o = 0$.

The maximum value of $G(\eta)$ is found at $G'(\eta) = o$, which is at

$$1 + 2\eta_c = e^{\eta_c}$$

solved by $\eta_c = 1.25643$. This is the same relation, for $F = G(\eta)$, for $\eta'' = 0$. Hence at η_c, $\eta''(\xi) = 0$ and $\eta'(\xi) = 0$.

When an $F > F_c$ ($\Gamma_i > \Gamma_{ic}$) is imposed, it is postulated that too many ions are injected relative to the electron injection, that the potential near the source rises and reflects some ions at a virtual anode. This is an easy physical concept, but is not allowed here analytically. The ions here are cold, all with the same velocity; the analysis needs changing for virtual anode formation, with a finite ion velocity distribution which allows for some ion flow to the plasma and for ions returning to the source.

COMBINING ZERO NET DENSITY and ZERO FIELD AT PLASMA

Let us combine the zero net charge density ($\eta''(\xi) = 0$) and the zero field ($\eta'(\xi) = 0$) information. We do this by plotting F for $\eta''(\xi) = 0$ (Figure 2) and F for $\eta(\xi) = 0$ and $\eta'(0) = 0$ (Figure 3) on the same axes, as appears in Figure 4. Let the former be $F \equiv F_D = e^{-\eta}\sqrt{\eta}$ and the latter be $F \equiv F_E = (1 - e^{-\eta}) / 2\sqrt{\eta}$. Then let us ask in what region are there solutions that fit the model at Figure 1? With the areas be denoted as shown, what do we observe?

areas B and C are where $(\eta'(0))^2 < 0$, not allowed here.

area D is where $(\eta'(0))^2 > 0$ (all right) but $\eta''(\xi) > 0$, which does not fit Figure 1.

area A is where $(\eta'(0))^2 > 0$ and $\eta''(\xi) < 0$, which does fit Figure 1

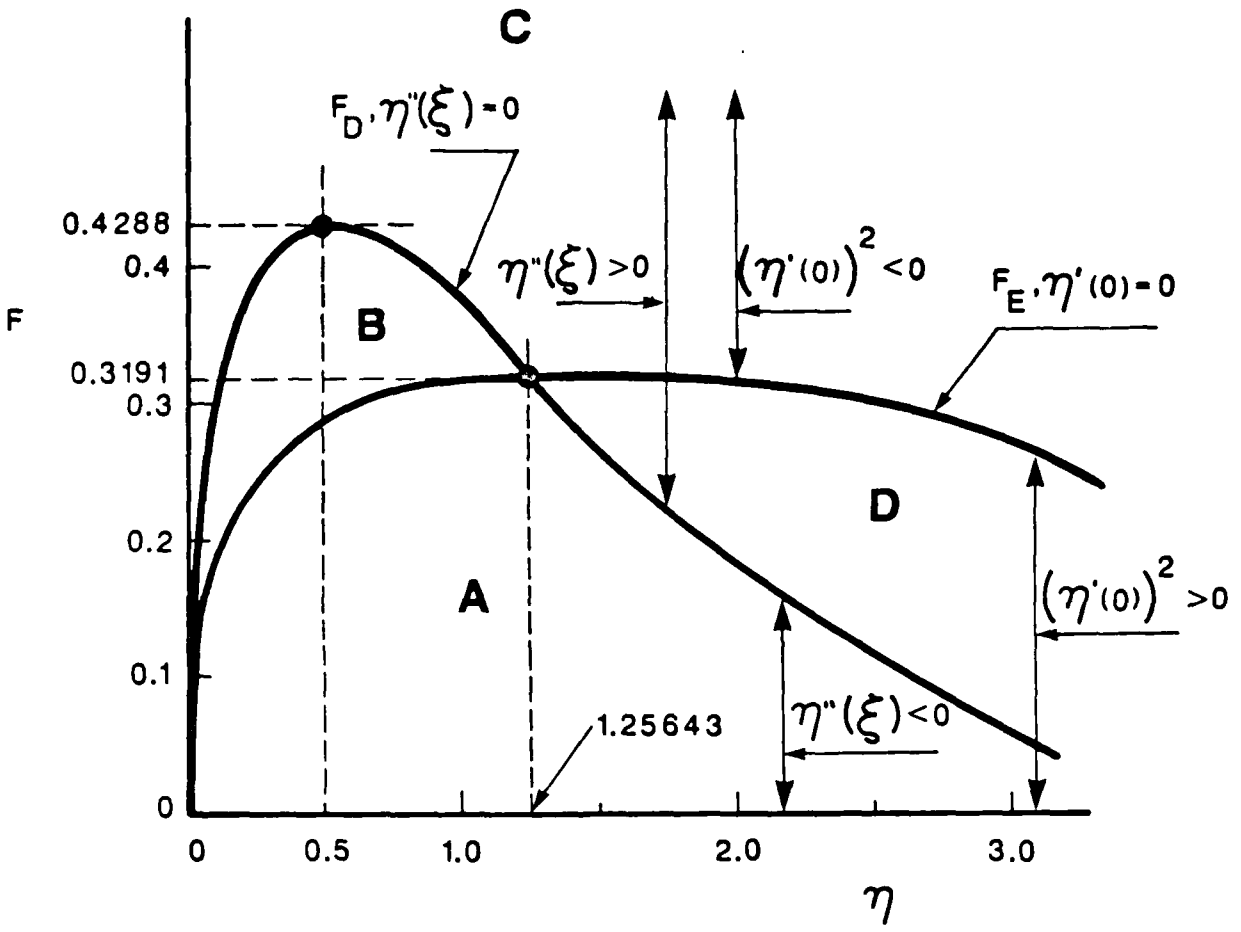

Figure 4. Combination of the ion flux F_D associated with zero net charge density at the plasma ($\eta''(\xi) = 0$) of Figure 2 with the ion flux F_E associated with zero electric field at the source. Only solutions in area A fit the assumed $\eta(\xi)$ shown in Figure 1. All of the above assumes $\eta'(\xi) = 0$, zero field at the plasma.

References

Bohm, D. "Minimum Ionic Kinetic Energy for a Stable Sheath," Chapter 3, pp. 77-86, in *Characteristics of Electrical Discharges in Magnetic Fields*,Ed. by A. Guthrie and R.K. Wakerling, McGraw-Hill (1949)

Harrison, E.R. and Thompson, W.B. "The Low Pressure Plane Symmetric Discharge," *Proc. Phys. Soc.* (London) **74** pp. 145-152 (1959)

Tonks, L. and Langmuir, I. "A General Theory of the Plasma of an Arc" *Phys. Rev.* **34** pp. 876-922 (1929)

SECTION II: PLASMA-WALL PHYSICS, THEORY AND SIMULATION

A. **Collector Sheath, Presheath, and Source Sheath in a Collisionless, Finite Ion Temperature Plasma**

Lou Ann Schwager

B. **Potential Drop and Transport in a Bounded Plasma with Ion Reflection at the Collector**

Lou Ann Schwager

C. **Potential Drop and Transport in a Bounded Plasma with Secondary Electron Emission at the Collector**

Lou Ann Schwager

Final reports with the above titles are in preparation for ERL memos and journal submissions. The final titles may be altered slightly.

D. **Magnetized Sheath; Kelvin-Helmholtz Instability; Long-lived Vortices**

Dr. Kim Theilhaber

A movie has been made displaying the long-lived vortices in detail. An ERL memorandum has been prepared to accompany the movie.

SECTION III: CODE DEVELOPMENT AND SOFTWARE DISTRIBUTION

Codes which we have developed or modified here are, generally speaking, available for the asking. We are making arrangements with our Industrial Liaison Program to handle distribution, at cost, of listings, tapes and/or diskettes. In a later report we will provide a list of codes and related material available and how to obtain such. If you use those, we simply ask that you acknowledge the source and also send us your results as published in reports or journals.

(Not all of the codes mentioned in our reports are available for distribution; some are single-purpose, single-user, too stylized for outside use.)

A. **A Relativistic Monte Carlo Binary Collision Model for Use in Plasma Particle Simulation Codes**

R. J. Procassini, C. K. Birdsall, E. C. Morse and B. I. Cohen

This report is to be issued as ERL Memorandum No. UCB/ERL M87-24, May 14, 1987. The introduction follows.

B. **Performance and Optimization of Direct Implicit Time Integration Schemes for Use in Electrostatic Particle Simulation Codes**

R. J. Procassini, C. K. Birdsall and E.C. Morse
and B. I. Cohen (Lawrence Livermore National Laboratory)

A. **A Relativistic Monte Carlo Binary Collision Model for U e in Plasma Particle Simulation Codes**

R. J. Procassini, C. K. Birdsall and E. C. Morse
and
B. I. Cohen (Lawrence Livermore National Laboratory)

1. Introduction

Particle simulations of plasma physics phenomena employ far fewer particles than the systems which are being simulated, owing to the limited speed and memory capacity of even the most powerful supercomputers. In practice, a system containing as many as 10^{20} particles is studied with upwards of 10^4 simulation particles. If the simulation consists of point particles in a gridless domain, then the combination of the small number of particles in a Debye sphere and the possibility of zero-impact-parameter, large-angle scattering results in a significant enhancement of fluctuation phenomena such as collisions.

In contrast, a gridded simulation has finite-size particles, due to the weighting or interpolation of the particles onto the grid and vice versa for the forces. These finite-size particles are tenuous in nature, being able to pass through each other. Therefore the interparticle force does not become singular as the distance of separation of the particle midpoints goes to zero, as it does for point particles.[1] This means that the average scattering angle for finite-size particle interactions is much smaller than that for point particle interactions, hence the collisionality for finite-size particles is reduced relative to that for point particles.

Accommodating collisional processes in a simulation may be difficult because

of disparate time scales. A comparison of the relevant physical time scales of the system that is being simulated usually yields a large range of values. For instance, the grid-cell transit time is usually several orders of magnitude smaller than the 90° scattering time. Much of the physical phenomena of interest in the simulation are due to these long-time-scale collisional processes[2], but short-time-scale processes (such as particle bounce times in a mirror or tokamak) must be adequately resolved if the plasma dielectric response and the plasma potential are to be accurately determined. This leads to important constraints on the modeling of binary collisions in our electrostatic particle simulation code **TESS** (**T**andem **E**xperiment **S**imulation **S**tudies).

In the following section we outline the physics and operation of the binary collision model within the electrostatic particle code. Section 3 presents the results of computer simulations of velocity space transport which were run to test the accuracy of the model. Finally, Section 4 discusses the timing statistics for the collision package relative to the other major physics packages in the code, as well as recommendations on the frequency of use of the collision package within the simulation sequence.

B. Performance and Optimization of Direct Implicit Time Integration Schemes for Use in Electrostatic Particle Simulation Codes

R. J. Procassini, C. K. Birdsall and E. C. Morse
and
B. I. Cohen (Lawrence Livermore National Laboratory)

1. Introduction

Implicit time integration schemes allow for the use of larger time steps than conventional explicit methods, thereby extending the applicability of kinetic particle simulation methods. This paper will describe a study of the performance and optimization of two such direct implicit schemes, which are used to follow the trajectories of charged particles in an electrostatic, particle-in-cell plasma simulation code. The two schemes that are studied were developed and analyzed by Langdon[1], and by Cohen, Langdon and Friedman[2]. The direct implicit method that was used for this study is an alternative to the moment-equation implicit method developed by Mason[3] and Denavit[4].

The organization of this paper is as follows: Section 2 will present the formulation of the two schemes, as well as the incorporation of these schemes into the particle simulation code. Section 3 will present the results of a numerical stability study of these schemes. This study is based upon the energy conservation, or lack thereof, of a freely expanding plasma slab in various regions of $\omega_{pe}\Delta t$, $\Delta x / \lambda_{De}$ parameter space, where ω_{pe} is the electron plasma frequency, λ_{De} is the electron Debye length, Δt is the time step and Δx is the grid spacing. Finally, Section 4

summarizes the results of this study, and gives suggestions for application of the results to the choice of a stable operating point for other types of plasma systems.

2. The Direct Implicit Electrostatic Particle Code

2.1 Direct Implicit Time Integration

The two implicit time integration schemes that were used for this study were chosen for their desirable properties. The most important of these are *i)* the relaxation of $\omega\Delta t$ constraints on the stability of the method, *ii)* strong damping of high-frequency modes for which $\omega\Delta t \gtrsim 1$, and *iii)* the second-order accuracy of the methods in the simulation of low-frequency phenomena for which $\omega\Delta t \lesssim 1$. These properties were originally studied through the normal-mode analysis of an electrostatic, cold-plasma oscillation in which the electrons undergo simple-harmonic oscillations.[2] The present study deals with one scheme from each of the C and D classes of schemes that are discussed in [2]. We will now briefly review the description of the C_1 and D_1 schemes.

2.1.1 The C_1 Scheme

The first multistep scheme that shall be considered for use in the time integration of the particle trajectories is of the form

$$\mathbf{x}_n = (C_0\mathbf{a}_n - C_1\mathbf{a}_{n-1} - \ldots - C_{k-2}\mathbf{a}_{n-k-2})\Delta t^2 - \mathbf{x}'_n \qquad (1a)$$

$$\mathbf{a}_{n-1} = (\mathbf{x}'_n - 2\mathbf{x}'_{n-1} - \mathbf{x}'_{n-2})\ \Delta t^2, \qquad (1b)$$

where $\mathbf{x}$ is the particle displacement, $\mathbf{x}'$ is the leapfrog particle displacement and $\mathbf{a}$ is the acceleration. The subscripts indicate the time step level of the variable. If $\mathbf{x}'$

is eliminated from the equations we get

$$(\mathbf{x}_n - 2\mathbf{x}_{n-1} + \mathbf{x}_{n-2})\,\Delta t^2 = \mathbf{a}_{n-1} + C_0(\mathbf{a}_n - 2\mathbf{a}_{n-1} + \mathbf{a}_{n-2}) + C_1(\mathbf{a}_{n-1} - 2\mathbf{a}_{n-2} + \mathbf{a}_{n-3}) + \ldots + C_k(\mathbf{a}_{n-k} - 2\mathbf{a}_{n-k-1} + \mathbf{a}_{n-k-2}) + \ldots. \quad (2)$$

This method is second-order accurate for small time step. The so-called C_1 scheme has the coefficients $C_s = 0$ for $s \geq 2$. A stability analysis for this scheme was performed by varying C_0 and C_1 independently, in an effort to determine the minimum value of $z \equiv exp(-i\omega\Delta t)$ for the least damped mode of a simple-harmonic oscillation at a frequency ω_0. The values of C_0 and C_1 at which these minima occur are $C_0 = 0.302$ and $C_1 = 0.040$, corresponding to an optimized scheme for which $z \sim 0.5$ as $\omega_0\Delta t \to \infty$. Therefore, the "optimized C_1 scheme" is given by

$$(\mathbf{x}_n - 2\mathbf{x}_{n-1} + \mathbf{x}_{n-2})\Delta t^2 = \mathbf{a}_{n-1} + 0.302(\mathbf{a}_n - 2\mathbf{a}_{n-1} + \mathbf{a}_{n-2}) + 0.040(\mathbf{a}_{n-1} - 2\mathbf{a}_{n-2} + \mathbf{a}_{n-3}). \quad (3)$$

2.1.2 The D_1 Scheme

The next multistep scheme that was used was derived from a classic second-order stiffly stable scheme for the solution of a first-order ordinary differential equation of the form $dy/dt = f(y,t)$. This multistep method is of the form

$$y_{n+1} - (4/3)y_n + (1/3)y_{n-1} = (2/3)f_{n+1}\Delta t. \quad (4)$$

The form of this equation motivates consideration of the more general class of second-order schemes which use $d\mathbf{x}/dt = \mathbf{v}$ and $d\mathbf{v}/dt = \mathbf{a}$ to produce

$$\mathbf{a}_{n+1}\Delta t^2 = d_0(\mathbf{x}_{n+1} - 2\mathbf{x}_n + \mathbf{x}_{n-1}) + d_1(\mathbf{x}_n - 2\mathbf{x}_{n-1} + \mathbf{x}_{n-2}) + \ldots. \quad (5)$$

In order to make this method second-order accurate, it was found that the coefficients $d_0, d_1, d_2, \ldots$ have to be chosen to satisfy the following two criteria

$$1 = d_0 - d_1 - d_2 - \ldots \tag{6a}$$

and

$$0 = d_0 - 2d_1 - 3d_2 - \ldots . \tag{6b}$$

The simplest of the class D algorithms has $d_s = 0$ for $s \geq 2$, such that from (6a) and (6b) we find that $d_0 = 2$ and $d_1 = -1$. This "D_1 scheme" is then given by

$$\mathbf{a}_{n-1}\Delta t^2 = 2\mathbf{x}_{n-1} - \mathbf{x}_n - \mathbf{x}_{n-1} - \mathbf{x}_{n-2}. \tag{7}$$

2.1.3 General Results and Properties

It was shown in [2] that relaxation of the $\omega_p \Delta t$ stability constraint in plasma simulation required the use of an implicit time integration scheme. This means that temporal resolution of the plasma frequency is forfeited to simulate lower frequency phenomena efficiently. This is particularly useful if the phenomenon of interest for the simulation is on a much slower time scale than that of plasma oscillations. Therefore, a time step that encompasses several plasma oscillation periods may be used in long time scale simulations while the scheme remains numerically stable. The coefficients that are used in the time integration schemes determine the degree of implicitness, the degree of high-frequency mode dissipation, and the stability of the scheme. When $\omega_0^2 \Delta t^2 \gg 1$, the high-frequency oscillations are distorted, even though the scheme remains stable. Therefore, the scheme should damp out

these distorted modes, while not affecting the low-frequency modes which are of interest. The z for the least damped simple-harmonic oscillator normal mode is plotted as a function of $\omega_0^2 \Delta t^2$, for both the C_1 and D_1 schemes in Figure 1. The figure shows that the damping for the D_1 scheme is stronger, and begins at smaller values of $\omega_0 \Delta t$, than that for the C_1 scheme. This is due to the fact that the only acceleration used in (7) is $\mathbf{a}_{n-1}$, indicating that the D_1 scheme attempts to force charge neutrality in only one time step as $\Delta t \rightarrow \infty$. In contrast, the C_1 scheme uses acceleration data from several previous time steps. Therefore, the C_1 scheme requires that more previous time step data be stored, than does the D_1 scheme. The storage of this data could become an important issue as the number of particles used in the simulation grows. The accuracy of the two schemes at low-frequencies was discussed in [2]. The weak damping of low-frequency oscillations indicated in Figure 1 yields high accuracy simulations in the "explicit" regime $\omega_0 \Delta t < 1$.

2.2 Electrostatic Field Equations

In addition to the implicit time integration of the particle trajectories, the calculation of the field quantities represents the other major implementation issue. The new position $\mathbf{x}_{n-1}$ was shown to depend upon the new acceleration $\mathbf{a}_{n-1}$ in the implicit time integration schemes. In an implicit electrostatic particle code, this acceleration is due to the new electric field $\mathbf{E}_{n-1}$. However, this field is not yet known, since it depends upon the charge density ρ_{n-1} and the particle position $\mathbf{x}_{n-1}$. Therefore, we have a large system of coupled, nonlinear particle and field equations that must be solved.

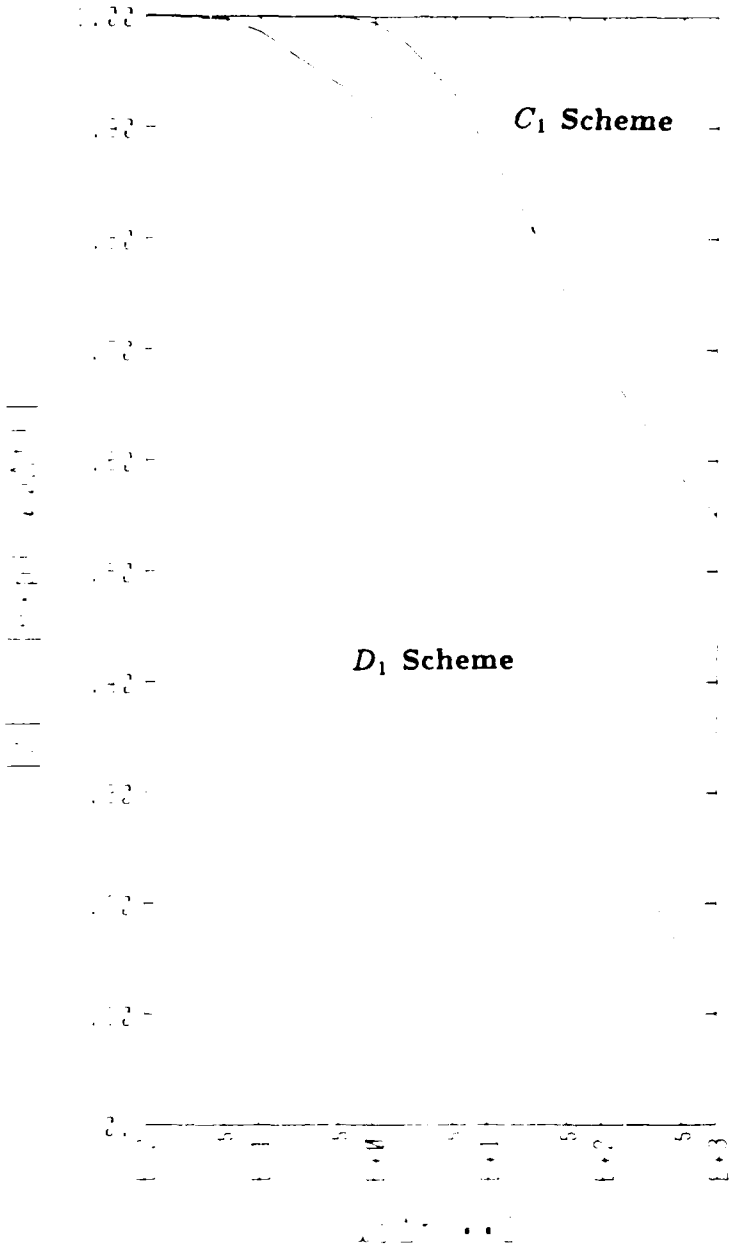

Figure 1. The absolute value of $z = exp(-i\omega\Delta t)$ of the least damped simple-harmonic oscillator normal mode versus $\omega_0^2\Delta t^2$ in the C_1 scheme (Eq. (3): dashed line) and the D_1 scheme (Eq. (7): dashed-dotted line).

One early method that was used to calculate the field quantities at the advanced time level involved the solution of a set of coupled field and fluid equations[3,4]. This is known as the implicit moment-equation method. In contrast, the direct implicit method uses a linearization of the particle-field equations to calculate the new electric field $\mathbf{E}_{n-1}$.

In general, the implicit time integration schemes described above give the new particle position as

$$\mathbf{x}_{n-1} = \beta\Delta t^2 \mathbf{a}_{n-1} + \tilde{\mathbf{x}}, \tag{8}$$

where $0 < \beta \leq 1$ is a constant of the time integration scheme and $\tilde{\mathbf{x}}$ is the explicitly computable "free-streaming" particle position , which is independent of $\mathbf{a}_{n-1}$. In an electrostatic code[5], $\mathbf{a}_{n-1}$ is due only to $\mathbf{E}_{n-1}$.

The new position $\mathbf{x}_{n-1}$ may be thought of as the explicitly computable position $\tilde{\mathbf{x}}$ plus a displacement $\delta\mathbf{x} = \beta\Delta t^2 \mathbf{a}_{n-1}$. The charge density is then taken as the sum of $\tilde{\rho}$ depending on the positions of $\tilde{\mathbf{x}}$, plus a linearized correction term due to the displacing of the particles by the amount $\delta\mathbf{x} = \mathbf{x}_{n-1} - \tilde{\mathbf{x}}$, which is equal to

$$\delta\rho = -\nabla \cdot [\tilde{\rho}(\mathbf{x})\delta\mathbf{x}(\mathbf{x})]. \tag{9}$$

The linearized displacement term

$$\delta\mathbf{x}(\mathbf{x}) \cong \beta\Delta t^2 q\mathbf{E}_{n-1}/m \tag{10}$$

then gives

$$\delta\rho(\mathbf{x}) = -\nabla \cdot [\chi(\mathbf{x})\mathbf{E}_{n-1}], \tag{11}$$

where the effective susceptibility is defined by

$$\chi(\mathbf{x}) = \beta q\tilde{\rho}(\mathbf{x})/m = \beta\omega_p^2\Delta t^2. \tag{12}$$

(These expressions have been generalized to the relativisitic case in our computer code **TESS**, which stands for **T**andem **E**xperiment **S**imulation **S**tudies). Poisson's equation is modified by the addition of this susceptibility to become, in rationalized cgs units

$$\nabla\cdot\mathbf{E_{n+1}} = \tilde{\rho} - \nabla\cdot(\chi\mathbf{E_{n+1}}) \tag{13}$$

or

$$-\nabla\cdot(1+\chi)\nabla\phi_{n+1} = \tilde{\rho}. \tag{14}$$

This form of the field equation depends only upon the particle position $\mathbf{x_{n+1}}$, as opposed to the implicit moment-equation method which also requires particle velocity information[5].

The **TESS** code uses a simplified finite difference form of (14), which in the absence of local spatial smoothing is given by:[5]

$$-(1+\bar{\chi}_j)\phi_{j+1} + (2+\bar{\chi}_j-\bar{\chi}_{j-1})\phi_j - (1+\bar{\chi}_{j-1})\phi_{j-1} = \tilde{\rho}_j\Delta x^2 \tag{15}$$

where

$$\bar{\chi}_j = (\chi_j + \chi_{j-1})/2 \tag{16}$$

is the midpoint effective susceptibility.

In the simulation of long time scale phenomena, it is desirable to have a value of $\omega_p^2\Delta t^2 \gg 1$, which means that $(1+\chi) \gg 1$, such that the field equation is

substantially different than Poisson's equation, which is the explicit limit of (14) for $\omega_p^2 \Delta t^2 \ll 1$.

3. Direct Implicit Method Performance Study

The performance of the C_1 and D_1 time integration schemes, as a function of location in $\omega_{pe}\Delta t$, $\Delta x / \lambda_{De}$ parameter space, was analyzed for the collisionless expansion of a one-dimensional, sharp boundary plasma slab into a vacuum. The free expansion of such plasma slabs has been previously discussed by Denavit[4,6], including a comparison of particle simulation results to a self-similar solution which assumes charge neutrality, isothermal electrons and cold ions. As the plasma expands into the vacuum due to the velocity of the particles, a rarefaction wave propagates into the plasma slab at the ion-acoustic speed c_s. The plasma density behind the wavefront falls off exponentially, and the ions are accelerated outward according to the velocity profile

$$v_{fi} = c_s + (x - x_0)/t \tag{17}$$

where v_{fi} is the velocity of the expanding ion front, x_0 is the location of the initial density discontinuity and x is the location of the ion front at time t. Figure 2 shows the electron and ion phase space plots for a typical expanding slab. The dashed line on the ion phase space plot (Figure 2b) represents the self-similar ion front velocity as given by (17). The agreement between the self-similar and particle simulation ion front velocities shown in Figure 2 was seen earlier in [6].

Freely expanding plasma slab simulations were made for various combinations of the important simulation parameters $\omega_{pe}\Delta t$ and $\Delta x / \lambda_{De}$ in the range

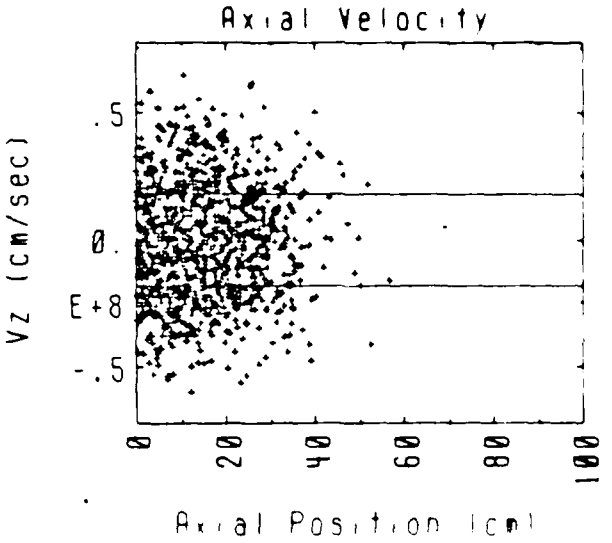

a) Electron Phase Space Distribution.

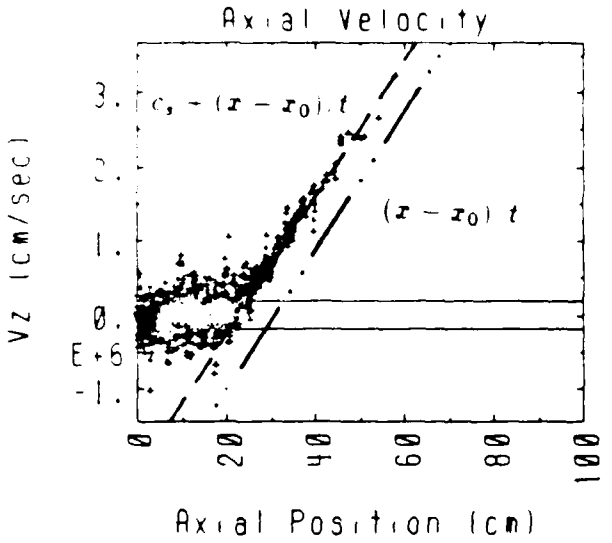

b) Ion Phase Space Distribution.

Figure 2. Phase space distributions for (a) electrons and (b) ions in the freely expanding plasma slab. The initial density discontinuity was located at $x_0 = 30.0cm$. The ions in the expansion region are accelerated due to the self-electric field. Note the agreement between the self-similar and particle simulation ion front velocities.

$0.1 \leq \omega_{pe}\Delta t \leq 200.0$, $0.1 \leq \Delta x\ \lambda_{De} \leq 100.0$, excluding the region for which $v_{the}\Delta t\ \Delta x > 2$. Several input parameters were the same for each of the simulations. These include the number of particles (2048 of each species), the mass ratio ($m_i\ m_e = 900$), the temperature ratio ($T_e\ T_i = 10$), the system half-width ($L = 100cm$), the initial plasma slab half-width ($L_{slab} = 30cm$) and the mesh size ($\Delta x = L\ 128 = 0.7843cm$). The values of ω_{pe} and Δx were the same for each of the simulations, while the temperature of the species (and hence λ_D) and Δt were varied.

In an attempt to quantify the performance of the two time integration schemes in various regions of $\omega_{pe}\Delta t$, $\Delta x\ \lambda_D$, parameter space, we employ the quantity $\Delta E\ E_0$ N, where ΔE is the change in the total plasma energy (kinetic plus electrostatic) through N time steps, normalized to the initial value of total plasma energy E_0. Figure 3 shows a typical time history of the total plasma energy for a simulation that resulted in numerical heating of the plasma. The freely expanding slab should exactly conserve energy, since the kinetic energy of the hot electrons is simply transferred to the cold ions through the self-electric field, resulting in the acceleration of the ions which was observed in Figure 2b. However, since **TESS** uses finite difference equations and the implicit algorithms described here are inherently dissipative, energy is *not* necessarily conserved. Some possible causes or mechanisms of non-conservation of energy include *a)* stochastic self-heating effects[7–9], *b)* self-heating effects arising from the interaction of spatial aliases, which are a consequence of the discrete nature of the grid, with the velocity distribution function of the particles[10] and *c)* numerical heating and cooling due to the dissipative nature of

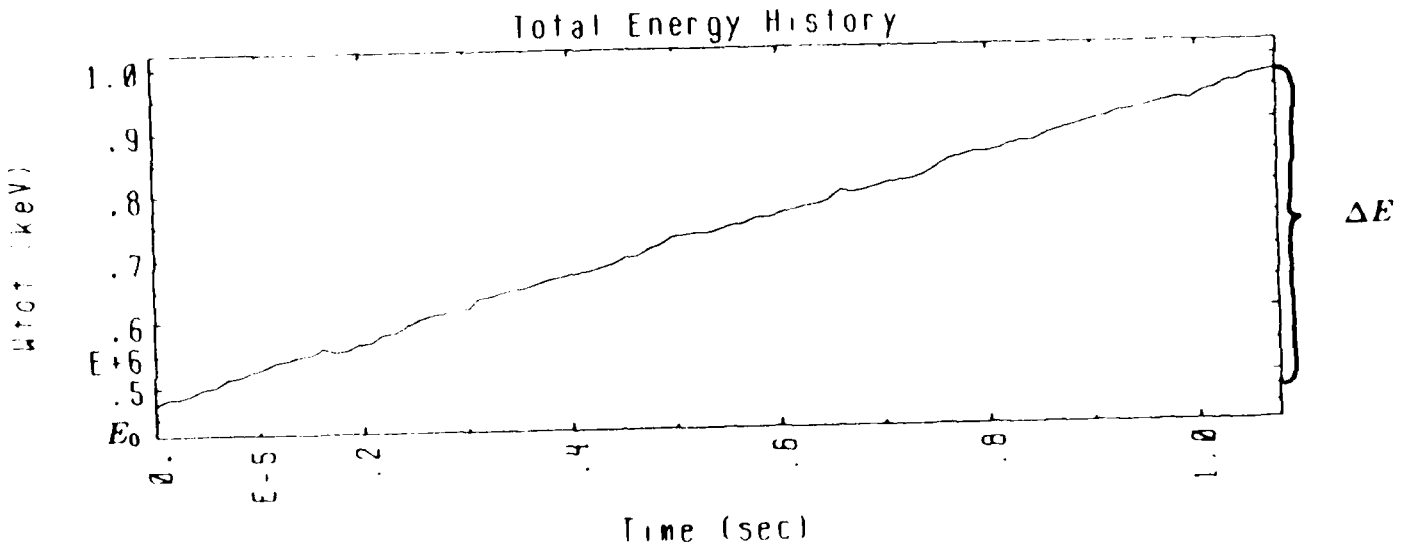

Figure 3. A typical time history plot of the total plasma energy for a simulation that resulted in numerical heating of the plasma.

the implicit time integration scheme[2]. This section presents the results of a study of the dependence of energy conservation on $\omega_{pe}\Delta t$ and $\Delta x / \lambda_{De}$ using the C_1 and D_1 implicit time integration schemes.

A set of 35 simulations were run for various combinations of $\omega_{pe}\Delta t$, $\Delta x / \lambda_{De}$ which span the aforementioned space. These runs were made using the C_1 and D_1 schemes, both with and without one-pass, local, self-consistent digital smoothing of (14) as described in detail in Section 3.3 of [5]. The spatial smoothing that was applied was of a simple, three-point, (1,2,1) form. It was therefore also possible to study the effect of spatial smoothing on the non-conservation of energy. The energy conservation results for these runs are given in Tables 1 and 2 for the C_1 scheme with and without spatial smoothing and in Tables 3 and 4 for the D_1 scheme with and without smoothing respectively. The data from these tables is shown in the contour plots of Figures 4 through 7.

The zero contour line on these figures indicates exact energy conservation, while positive (negative) contour lines indicate numerical heating (cooling) of the plasma. (The positive contour lines are solid, the negative contour lines are dashed, the zero contour line is the bold solid curve and the $v_{th_e}\Delta t / \Delta x = 1$ line is the bold dashed line). The filled circles show the locations in $\omega_{pe}\Delta t$, $\Delta x / \lambda_{De}$ parameter space at which the simulations were run. The coarse nature of the contour lines is due to the limited number of runs in the simulation set. The space could be extended to larger values of the two parameters, but the cost of each run increases rapidly as $\Delta x / \lambda_{De}$ is increased, due to the decreasing particle thermal velocity, which in turn

Table 1

Energy Conservation for the C_1 Scheme without Spatial Smoothing in $\omega_{pe}\Delta t$, $\Delta x / \lambda_{De}$ Parameter Space

$\omega_{pe}\Delta t$	$\Delta x / \lambda_{De}$	$(\Delta E / E_0)\ N$
0.1	0.1	0.0
0.1	1.0	0.0
0.1	5.0	9.4×10^{-5}
0.1	10.0	5.4×10^{-4}
0.1	30.0	5.8×10^{-3}
0.1	50.0	1.2×10^{-2}
0.1	100.0	1.3×10^{-2}
0.2	0.1	-5.8×10^{-4}
1.0	1.0	-1.7×10^{-4}
1.0	5.0	4.1×10^{-4}
1.0	10.0	2.8×10^{-3}
1.0	30.0	2.7×10^{-2}
1.0	50.0	6.2×10^{-2}
1.0	100.0	5.9×10^{-2}
2.0	1.0	1.0×10^{-3}
5.0	5.0	6.3×10^{-3}
5.0	10.0	2.1×10^{-4}
5.0	30.0	5.2×10^{-3}
5.0	50.0	2.0×10^{-2}
5.0	100.0	8.1×10^{-2}

Table 1 (continued)

$\omega_{pe}\Delta t$	$\Delta x / \lambda_{De}$	$(\Delta E / E_0)/N$
10.0	5.0	2.1×10^{-1}
10.0	10.0	9.6×10^{-3}
10.0	30.0	1.4×10^{-3}
10.0	50.0	4.8×10^{-3}
10.0	100.0	2.3×10^{-2}
20.0	10.0	1.2×10^{0}
30.0	30.0	4.0×10^{-2}
30.0	50.0	9.7×10^{-5}
30.0	100.0	2.0×10^{-3}
50.0	50.0	1.6×10^{-1}
50.0	100.0	2.8×10^{-4}
60.0	30.0	4.8×10^{-1}
100.0	50.0	1.1×10^{0}
100.0	100.0	1.6×10^{-1}
200.0	100.0	3.1×10^{0}

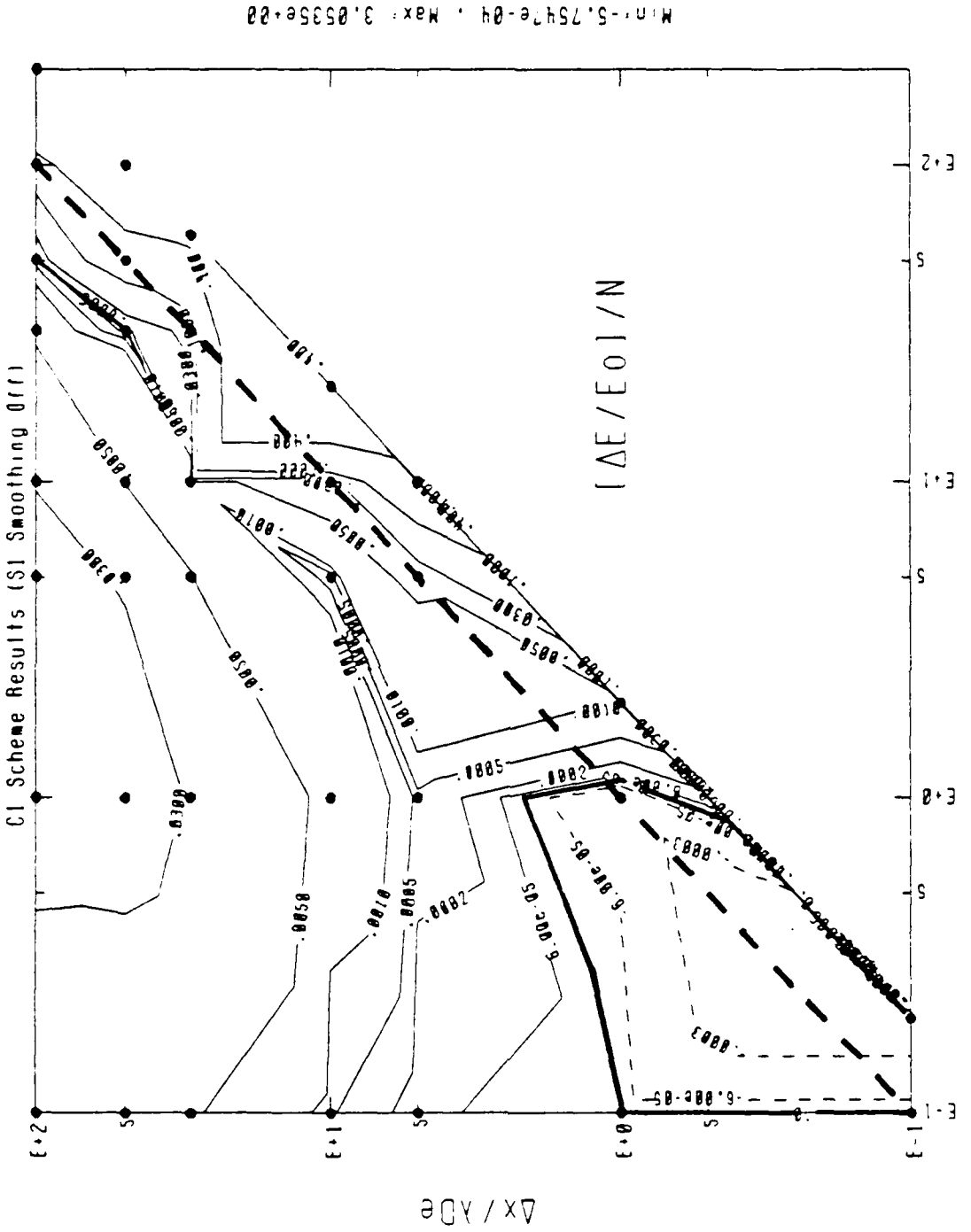

Figure 4. Contour plots of $(\Delta E/E_0)/N$ as a function of $\omega_{pe}\Delta t$ and $\Delta x/\lambda_{De}$ for the C_1 Scheme without Spatial Smoothing. The zero contour indicates exact conservation of energy.

Table 2

Energy Conservation for the C_1 Scheme with Spatial Smoothing in $\omega_{pe}\Delta t$, $\Delta x / \lambda_{De}$ Parameter Space

$\omega_{pe}\Delta t$	$\Delta x / \lambda_{De}$	$(\Delta E / E_0) / N$
0.1	0.1	0.0
0.1	1.0	0.0
0.1	5.0	2.2×10^{-5}
0.1	10.0	1.5×10^{-4}
0.1	30.0	8.0×10^{-4}
0.1	50.0	3.8×10^{-4}
0.1	100.0	2.0×10^{-4}
0.2	0.1	-5.8×10^{-4}
1.0	1.0	-1.2×10^{-4}
1.0	5.0	9.2×10^{-5}
1.0	10.0	7.9×10^{-4}
1.0	30.0	5.6×10^{-3}
1.0	50.0	4.5×10^{-3}
1.0	100.0	2.8×10^{-3}
2.0	1.0	5.6×10^{-4}
5.0	5.0	1.9×10^{-3}
5.0	10.0	2.5×10^{-5}
5.0	30.0	3.1×10^{-3}
5.0	50.0	1.1×10^{-2}
5.0	100.0	2.7×10^{-2}

Table 2 (continued)

$\omega_{pe}\Delta t$	$\Delta x / \lambda_D$	$\Delta E / E_0 N$
10.0	5.0	3.1×10^{-1}
10.0	10.0	6.0×10^{-3}
10.0	30.0	1.1×10^{-3}
10.0	50.0	3.7×10^{-3}
10.0	100.0	1.5×10^{-2}
20.0	10.0	3.8×10^{-1}
30.0	30.0	3.3×10^{-2}
30.0	50.0	0.0
30.0	100.0	1.7×10^{-3}
50.0	50.0	2.0×10^{-1}
50.0	100.0	-7.6×10^{-5}
60.0	30.0	4.3×10^{-1}
100.0	50.0	5.7×10^{-1}
100.0	100.0	1.8×10^{-1}
200.0	100.0	6.7×10^{0}

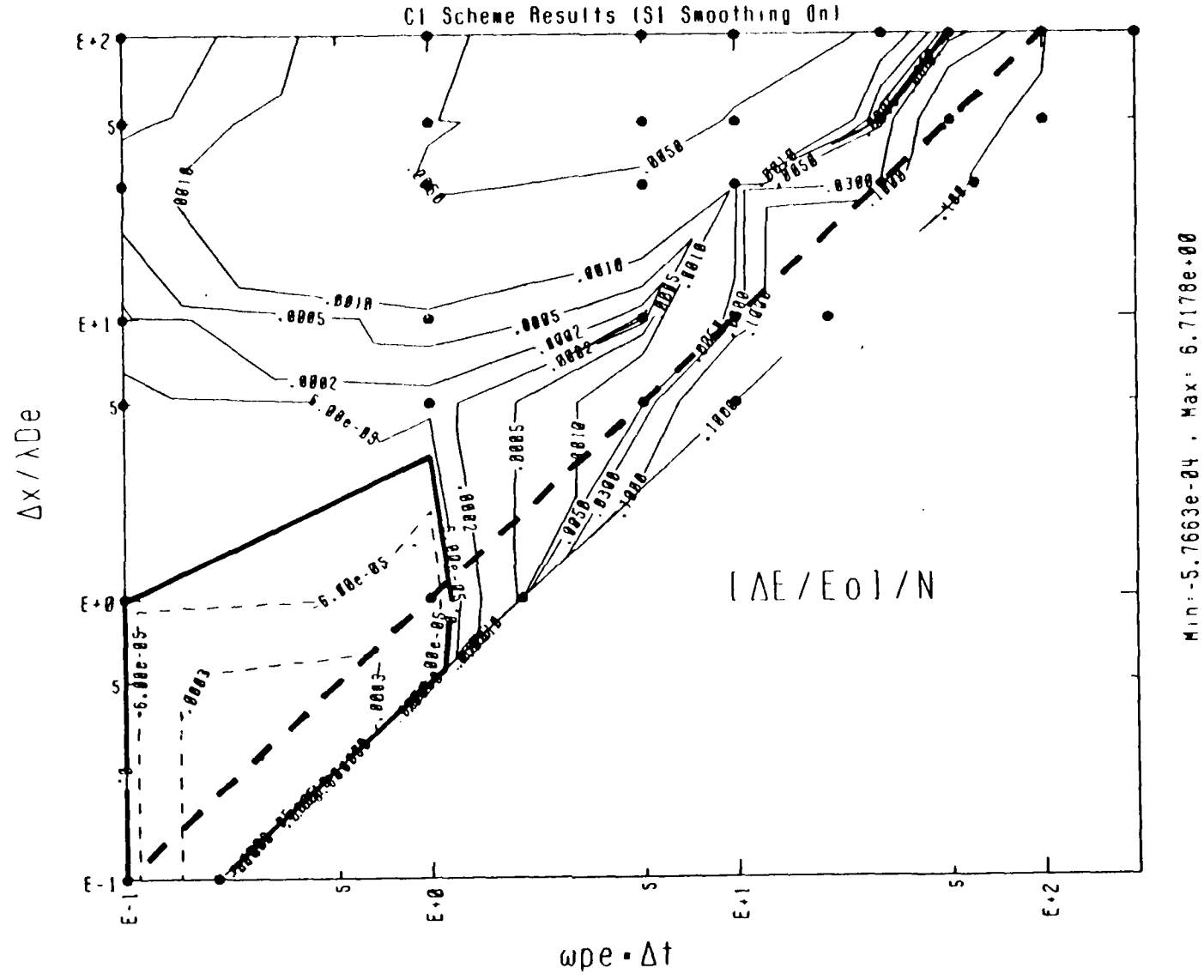

Figure 5. Contour plots of $(\Delta E/E_0)/N$ as a function of $\omega_{pe}\Delta t$ and $\Delta x/\lambda_{De}$ for the C_1 Scheme with Spatial Smoothing. The zero contour indicates exact conservation of energy.

requires a greater number of time steps for a uniform expansion of the slab among all of the runs.

Explicit particle simulation codes are usually limited to operation in the lower left hand region above the bold dashed line. The direct implicit method greatly extends this region of operation. The figures indicate that it is possible to use large values of $\omega_{pe}\Delta t$ and $\Delta x / \lambda_{De}$ which result in negligible or no loss of energy conservation. Therefore, one may increase the cost effectiveness of the simulation by employing a time step which is larger than the electron plasma period, while accurately simulating the low-frequency phenomena of interest, such as MHD (in implicit electromagnetic codes) and particle transport. It must be stressed that the results presented here are applicable for either periodic plasma systems or systems in which the plasma is not in contact with a wall. The effect of potential sheaths near a surface may yield different conclusions regarding regions of numerical heating and cooling than those presented here.

The contour plots for the C_1 scheme, Figures 4 and 5, show that energy is conserved up to maximum values of $\Delta x / \lambda_{De} \approx 3$ and $\omega_{pe}\Delta t \approx 1$. For larger values of these parameters, there is numerical heating, while smaller values lead to numerical cooling of the plasma. The addition of local spatial smoothing allows the zero contour line to extend to slightly larger values of the two parameters. Smoothing also reduces the numerical heating at large values of $\Delta x / \lambda_{De}$ by about a factor of 4. The data points at $\omega_{pe}\Delta t = 200.0$, $\Delta x / \lambda_{De} = 100.0$ are subject to very rapid numerical heating with the C_1 scheme. Spatial smoothing increases the

heating rate at this point, which is the opposite effect to that seen in other regions of the parameter space.

In contrast to the contour plots for the C_1 scheme, Figures 6 and 7 indicate that there are regions in the space with large values of $\omega_{pe}\Delta t$ and $\Delta x / \lambda_{De}$ for which the energy of the system is conserved well when the D_1 scheme is used. The zero contour line lies approximately parallel to the $v_{the}\Delta t / \Delta x \approx 1$ (bold dashed) line, and extends out to $\omega_{pe}\Delta t \approx 30$, $\Delta x / \lambda_{De} = 100$ following a path described approximately by $v_{the}\Delta t / \Delta x \approx 0.30 \pm 0.13$ for $\omega_{pe}\Delta t \gtrsim 1$. This behavior may continue to larger values of the two parameters, which would allow for very large time step simulations in which numerical heating and cooling are not significant. Note that there is a very rapid rate of change in $(\Delta E / E_0) / N$ about the zero contour line, especially for $\omega_{pe}\Delta t \gtrsim 1$. Spatial smoothing yields approximately a factor of 3 reduction in the numerical heating at large values of $\Delta x / \lambda_{De}$. The smoothing also results in numerical heating for small values of the two parameters, which is the opposite of the results obtained without any spatial smoothing.

4. Conclusions

The C_1 and D_1 direct implicit time integration schemes have been shown to extend the region of operation for which the total plasma energy is conserved beyond that which is applicable for an explicit time integration scheme. The C_1 scheme was found to have a limited region of parameter space over which energy is well conserved. The D_1 scheme possesses a much larger region of parameter space for good energy conserving operation. In fact, for the range of parameter space $0.1 \leq \omega_{pe}\Delta t \leq 200.0$, $0.1 \leq \Delta x / \lambda_{De} \leq 100.0$, the D_1 scheme was shown to conserve

Table 3

Energy Conservation for the D_1 Scheme without Spatial Smoothing in $\omega_{pe}\Delta t$, $\Delta x / \lambda_{De}$ Parameter Space

$\omega_{pe}\Delta t$	$\Delta x / \lambda_{De}$	$(\Delta E / E_0) / N$
0.1	0.1	0.0
0.1	1.0	-5.2×10^{-6}
0.1	5.0	7.9×10^{-5}
0.1	10.0	5.4×10^{-4}
0.1	30.0	5.0×10^{-3}
0.1	50.0	8.3×10^{-3}
0.1	100.0	1.4×10^{-2}
0.2	0.1	-7.5×10^{-4}
1.0	1.0	-7.8×10^{-4}
1.0	5.0	*0.0*
1.0	10.0	1.2×10^{-3}
1.0	30.0	1.7×10^{-2}
1.0	50.0	3.6×10^{-2}
1.0	100.0	6.7×10^{-2}
2.0	1.0	-2.0×10^{-3}
5.0	5.0	-1.9×10^{-3}
5.0	10.0	-7.3×10^{-4}
5.0	30.0	1.2×10^{-3}
5.0	50.0	-5.9×10^{-3}
5.0	100.0	2.4×10^{-2}

Table 3 (continued)

$\omega_{pe}\Delta t$	$\Delta x/\lambda_{De}$	$(\Delta E/E_0)/N$
10.0	5.0	-4.3×10^{-3}
10.0	10.0	-3.0×10^{-3}
10.0	30.0	-5.7×10^{-5}
10.0	50.0	8.7×10^{-4}
10.0	100.0	5.7×10^{-3}
20.0	10.0	-6.9×10^{-3}
30.0	30.0	-3.5×10^{-3}
30.0	50.0	-1.6×10^{-3}
30.0	100.0	-3.9×10^{-4}
50.0	50.0	-4.2×10^{-3}
50.0	100.0	-2.2×10^{-3}
60.0	30.0	-9.4×10^{-3}
100.0	50.0	-8.4×10^{-3}
100.0	100.0	-4.5×10^{-3}
200.0	100.0	-7.5×10^{-3}

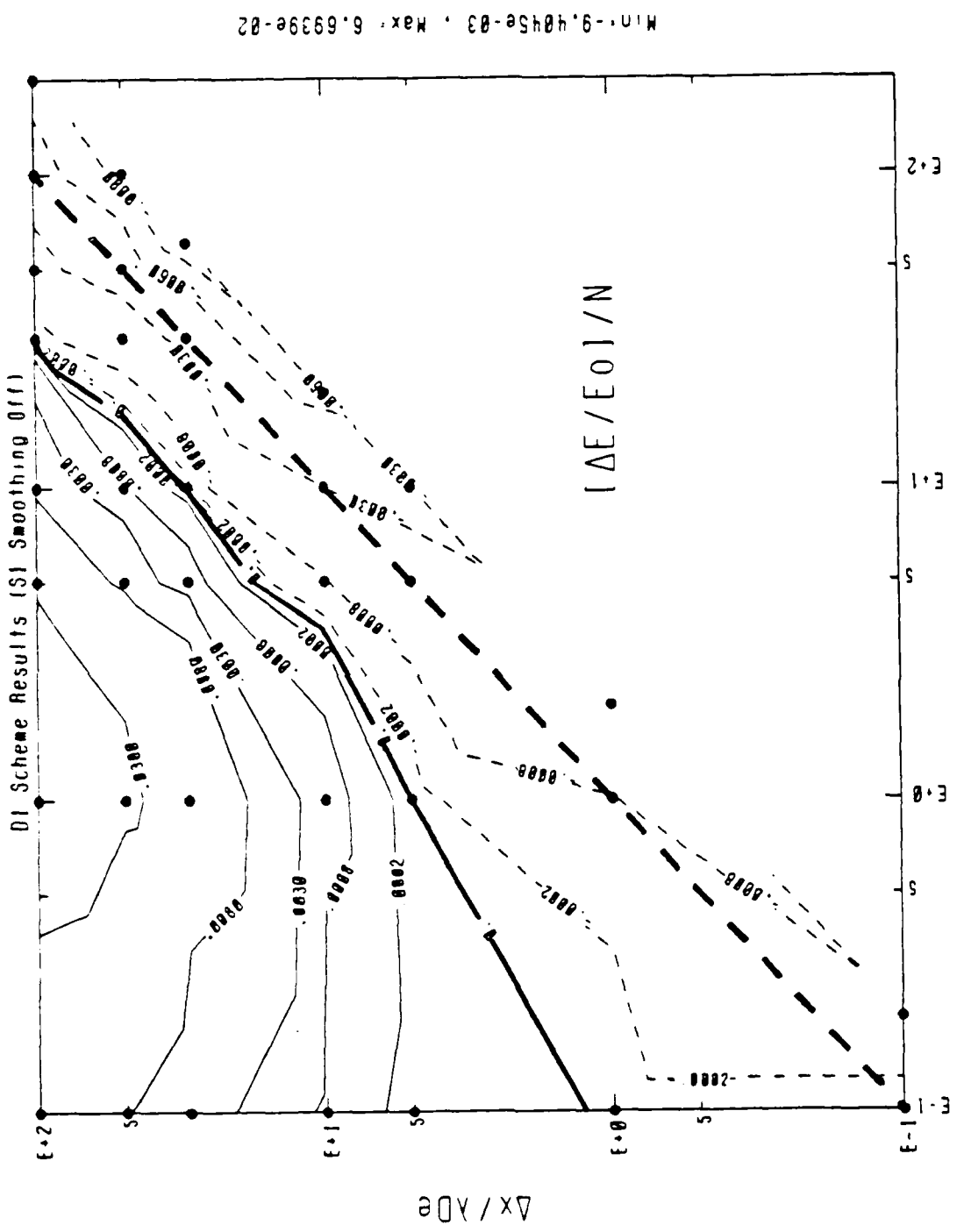

Figure 6. Contour plots of $(\Delta E/E_0)/N$ as a function of $\omega_{pe}\Delta t$ and $\Delta x/\lambda_{De}$ for the D_1 Scheme without Spatial Smoothing. The zero contour indicates exact conservation of energy.

Table 4

Energy Conservation for the D_1 Scheme with Spatial Smoothing in $\omega_{pe}\Delta t$, $\Delta x/\lambda_{De}$ Parameter Space

$\omega_{pe}\Delta t$	$\Delta x/\lambda_{De}$	$(\Delta E/E_0)/N$
0.1	0.1	0.0
0.1	1.0	0.0
0.1	5.0	2.0×10^{-5}
0.1	10.0	1.6×10^{-4}
0.1	30.0	8.5×10^{-4}
0.1	50.0	3.5×10^{-4}
0.1	100.0	2.0×10^{-4}
0.2	0.1	-7.5×10^{-4}
1.0	1.0	-7.0×10^{-4}
1.0	5.0	-7.4×10^{-5}
1.0	10.0	2.4×10^{-4}
1.0	30.0	3.5×10^{-3}
1.0	50.0	3.1×10^{-3}
1.0	100.0	2.1×10^{-3}
2.0	1.0	-2.1×10^{-3}
5.0	5.0	-1.9×10^{-3}
5.0	10.0	-8.0×10^{-4}
5.0	30.0	6.8×10^{-4}
5.0	50.0	2.6×10^{-3}
5.0	100.0	8.7×10^{-3}

Table 4 (continued)

$\omega_{pe}\Delta t$	$\Delta x / \lambda_{De}$	$(\Delta E / E_0) / N$
10.0	5.0	-5.1×10^{-3}
10.0	10.0	-3.1×10^{-3}
10.0	30.0	-1.6×10^{-4}
10.0	50.0	7.7×10^{-4}
10.0	100.0	4.0×10^{-3}
20.0	10.0	-7.1×10^{-3}
30.0	30.0	-3.5×10^{-3}
30.0	50.0	-1.7×10^{-3}
30.0	100.0	-5.8×10^{-4}
50.0	50.0	-4.2×10^{-3}
50.0	100.0	-2.1×10^{-3}
60.0	30.0	-8.8×10^{-3}
100.0	50.0	-8.4×10^{-3}
100.0	100.0	-4.5×10^{-3}
200.0	100.0	-9.6×10^{-3}

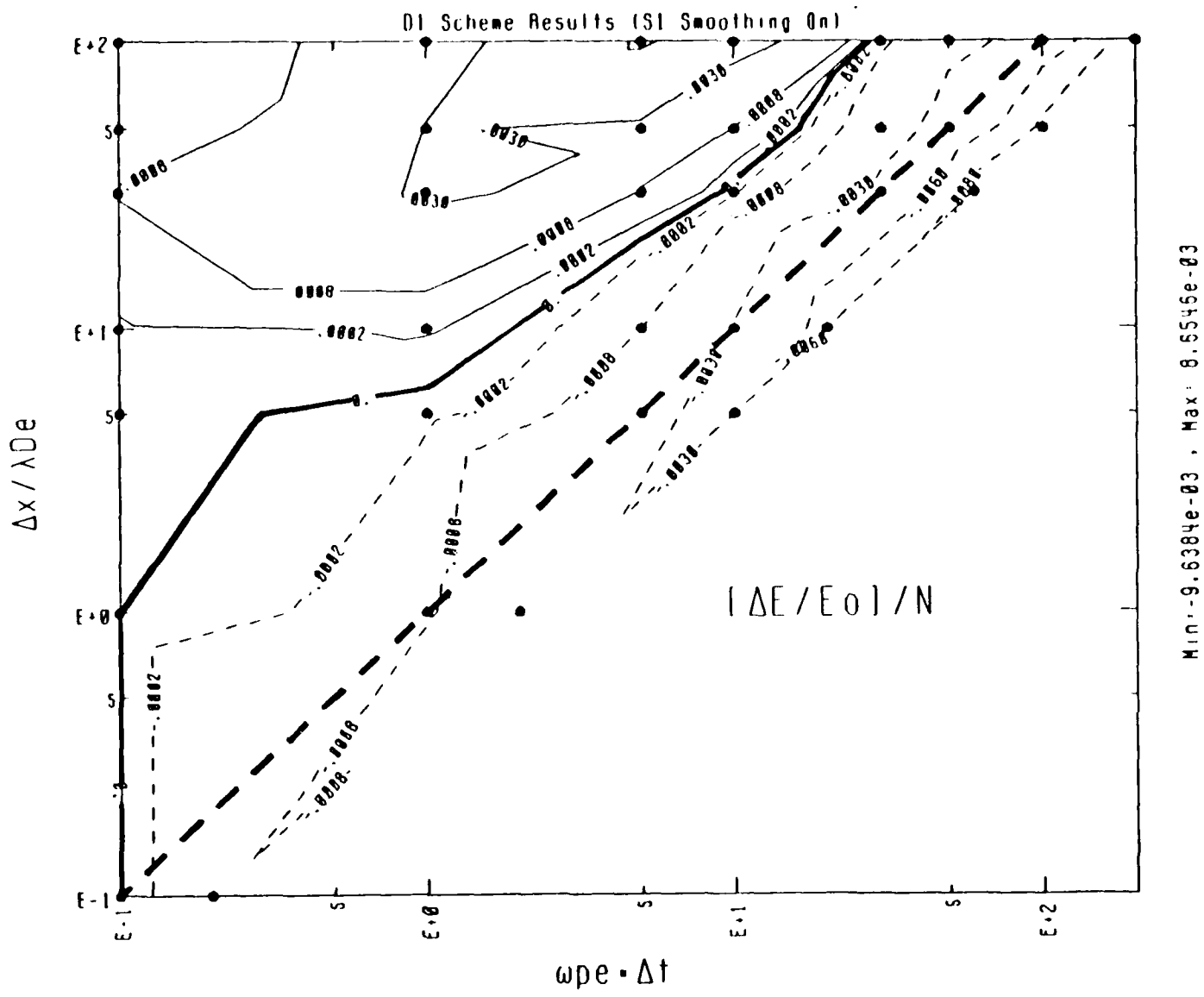

Figure 7. Contour plots of $(\Delta E/E_0)/N$ as a function of $\omega_{pe}\Delta t$ and $\Delta x/\lambda_{De}$ for the D_1 Scheme with Spatial Smoothing. The zero contour indicates exact conservation of energy.

energy well along a path described by $v_{the}\Delta t/\Delta x \approx 0.30 \pm 0.13$. Numerical heating was found for large values of $\Delta x / \lambda_{De}$ with each of the schemes. The amount of heating in a given region of the space was found to be comparable between the two schemes, with the D_1 scheme heating slightly less than the C_1 scheme. Numerical cooling of the plasma system was found for the lowest values of the parameters in the space, except when the D_1 scheme was used with local spatial smoothing. Spatial smoothing generally yielded a factor of 3 to 4 reduction in the amount of numerical heating, and a slight decrease in the amount of numerical cooling relative to the same simulation run without smoothing. The smoothing did not substantially alter the gross topology of the energy conservation plots.

If low-frequency phenomena are of interest, as opposed to high-frequency effects, the large degree of high-frequency damping provided by the D_1 scheme (see Figure 1) will allow the use of time steps that encompass several electron plasma periods. The $\omega_{pe}\Delta t$ time step constraint is thereby relaxed, resulting in an increased cost effectiveness of the simulation. For such simulations, the D_1 scheme is more desirable for use than the C_1 scheme. Since the energy conservation contour plot for the D_1 scheme has a steep gradient about the energy conserving contour, care must be taken to ensure that the operation point is chosen as close to the energy conserving contour as possible.

The results presented here are for a freely expanding, bounded plasma slab. The conclusions that are drawn from these results are probably applicable to other plasma systems. A similar performance study should be undertaken for systems

in which the plasma is in contact with a wall, in order to determine the numerical performance of such simulations using these direct implicit schemes.

References

[1] A. B. Langdon, *J. Comput. Phys* **30**, 202(1979).

[2] B. I. Cohen, A. B. Langdon and A. Friedman, *J. Comput. Phys.* **46**, 15(1982).

[3] R. J. Mason, *J. Comput. Phys.* **41**, 223(1981).

[4] J. Denavit, *J. Comput. Phys.* **42**, 337(1981).

[5] A. B. Langdon, B. I. Cohen and A. Friedman, *J. Comput. Phys.* **51**, 107(1983).

[6] J. Denavit, *Phys. Fluids* **22**, 1384(1979).

[7] R. W. Hockney, *J. Comput. Phys.* **8**, 19(1971).

[8] A. Peiravi and C. K. Birdsall, *Proc. Eighth Conf. Num. Sim. Plasmas*, PD-9, Monterey, Calif., 28-30 June 1978.

[9] C. K. Birdsall and A. B. Langdon, **Plasma Physics via Computer Simulation**, Pages 293-295, McGraw-Hill, New York(1985).

[10] A. B. Langdon, *J. Comput. Phys.* **6**, 247(1970).

SECTION IV: JOURNAL ARTICLES, REPORTS, TALKS, VISITS

Journal Articles

S. Kuhn and M. Hörhager, "External-circuit Effects on Pierce-diode Stability Behavior," *Journal of Applied Physics*, Vol. 60, No. 6, September 15, 1986, pp. 1952-1959.

Alex Friedman, R. N. Sudan, Jacques Denavit, "Stability of Field-reversed Ion Rings," *Physics of Fluids*, Vol. 29, No. 10, October, 1986, pp.3317-3341.

Reports

Niels F. Otani and Bruce I. Cohen, "Effect of Large-Amplitude Perpendicularly-Propagating RF Waves on the Interchange Instability," University of California, Berkeley, Memorandum No. UCB/ERL M86/48, July 8, 1986.

William S. Lawson, "Linear Magnetized Plasma Response to an Oblique Electrostatic Wave," University of California, Berkeley, Memorandum No. UCB/ERL M86/94, December 15, 1986

Poster Papers presented at American Physical Society, Twenty-Eighth Annual Meeting, Division of Plasma Physics, Baltimore, Maryland, November 3-7, 1986 (abstracts follow).

T. L. Crystal and S. Kuhn, "Pierce Diode Instability with External Inductance and Resistance"

L. A. Schwager and C. K. Birdsall, "Transport across the Plasma-Wall Sheath with Secondary Electron Emission and Ion Reflection"

S. E. Parker, C. K. Birdsall and K. Theilhaber, "Electrostatic Effects on Confinement Outside the Separatrix of Field Reverse Configurations"

R. J. Procassini, C. K. Birdsall, and B. I. Cohen, "Direct Implicit Particle Simulation of Tandem Mirrors"

K. Theilhaber and C. K. Birdsall, "Structure of the Crossed-Field Sheath," (with short movie)

Talks

C. K. Birdsall and the Plasma Theory and Simulation Group, "Planar Plasma Discharges: Simulations and Experiments," at Sandia National Labs, October 7, 1986

C. K. Birdsall, "Some Aspects of Plasma Simulation Using Many Particles (moving 10^6 particles per second on a Cray)," University of California, Berkeley, Center for Pure and Applied Mathematics, October 16, 1986.

C. K. Birdsall and Michael Lieberman, "Planar Plasma Discharges: Simulations and Experiments" at Varian Associates Technical Seminar, October 20, 1986.

Visitors

Dr. G. Emmert, University of Wisconsin, August 4
Dr. M.J. Gerver, Massachusetts Institute of Technology, Aug. 4-11
Dr. T. L. Crystal, Palo Alto, July 1-September 30
Dr. S. Kuhn, University of Innsbruck, July 1-September 30

Workshop

Bounded-Plasma Physics Workshop, University of California, Berkeley, September 22-23, 1986 (see schedule following).

Pierce Diode Instability Simulations with External Inductance and Resistance -- T.L. Crystal and S. Kuhn, *U.C.Berkeley, Electronics Research Laboratory*. The classical Pierce diode is a bounded plasma with an external short circuit; the linear instability analysis[1] of the classical equilibrium was verified using 1D1v particle simulations[2]. Linear analysis of the extended Pierce diode [meaning the same uniform equilibrium but with finite external circuit R or L] predicts significant departures from the classical case in terms of instability thresholds, growth rates, and the physical nature of the instability. The peculiarities of these extended Pierce diode eigenfrequencies and corresponding field profiles have now also been examined with particle simulations.

* Work supported by ONR contract N00014-85-K-0809, and by Austrian Research Funds.

1. S. Kuhn, *Phys. Fluids* **27**, 1834 (1985).
2. T.L. Crystal and S. Kuhn, *Phys. Fluids* **28**, 2116 (1985).

Transport across the Plasma-Wall Sheath with Secondary Electron Emission and Ion Reflection. L.A.Schwager and C.K.Birdsall, U.C. Berkeley* -- Particle and energy transport from a warm plasma to a floating wall is obtained with electrostatic particle simulations in 1d. The wall may emit secondary electrons or reflect ions. For both boundary effects, we find that the collected electrons carry an average energy to the plate equal to the bulk plasma temperature (kT per electron) even though T_e drops by two in the sheath. As the ion reflection fraction increases, the reflected current increases the plasma density which then increases the ion energy flux to the collector. Even with an ion-ion two-streaming instability, the time-averaged values of transport results agree with time-independent analysis. Increasing secondary emission beyond where E_n reverses increases potential fluctuations and causes departure from time-independent theory,[1] especially for cool secondaries.

*Work supported by DOE contract 1-442427-22401.

[1]G.D.Hobbs and J.A.Wesson, Plasma Physics, 9, 1967

Electrostatic Effects on Confinement Outside The Separatrix of Field Reverse Configurations, S. E. Parker, C. K. Birdsall, and K. Theilhaber, UC-Berkeley*--A two dimensional particle code is being used to study the formation of electrostatic potentials due to magnetic peaks and wells with an injected flux of well magnetized electrons and weakly magnetized ions. Electrostatic effects may explain the enhanced plasma confinement observed in the open field line region of the FRC[1]. Experimental results have shown the formation of large potentials due to nonuniform magnetic fields. This type of phenomena is being modelled. We are seeking to show that magnetic wells cause the formation of potential peaks and magnetic peaks form potential wells when ions are weakly magnetized compared to the electrons. These results will be used to interpret the electrostatic potential contour of the open field line region in the FRC.

1. L. E. Steinhauer, "Enhanced Confinement Outside the Separatrix of FRC's", Spectra Technology, Inc., (1986).

* Work supported by DOE contract FG03-86ER53220

Direct Implicit Particle Simulation of Tandem Mirrors.* R. J. PROCASSINI, C. K. BIRDSALL,† and B. I. COHEN, Lawrence Livermore National Laboratory--We developed TESS, a one-dimensional (axial), relativistic, electrostatic particle code to simulate thermal barrier formation and ambipolar potential particle confinement in one-half of a symmetric tandem mirror plasma. Our recent advances in TESS development include: optimization studies of two direct implicit, finite difference schemes yielding operating regimes of relative numerical stability (i.e., no numerical heating or cooling) in $\omega_{pe}\Delta t$ vs $\Delta x/\lambda_{de}$ parameter space for each scheme; calculations (in the absence of auxiliary heating) of ambipolar potential of a collisionless plasma in a non-uniform, tandem mirror magnetic field with non-reflecting, no-axial-loss boundary conditions; incorporation into TESS of a relativistic, energy and momentum conserving, Monte Carlo binary particle collision algorithm. We will also review our implementation of algorithms for rf and neutral beam auxiliary heating, axial and radial particle losses, and plasma fueling.

*Work supported by the USDOE under Cont. W-7405-ENG-48.

†University of California, Berkeley, CA.

Structure of the Crossed-Field Sheath - K. Theilhaber and C.K. Birdsall, University of California, Berkeley.

We consider the equilibrium and time-dependent behavior of the plasma-wall sheath which is formed when the external magnetic field is parallel to the wall. The presence of the material boundary initially creates a layer of charge depletion near the surface, of thickness comparable to the ion gyro-radius. This results in a strongly nonuniform electric field which induces a sheared $\underline{E} \times \underline{B}$ motion of ions and electrons parallel to the wall. Physical arguments as well as analytical and numerical studies of a similar but unbounded configuration(1) suggest that this flow is subject to the Kelvin-Helmholtz instability, with a long-term evolution into a set of vortices separating the boundary from the plasma. We shall present an analytical model for the instability, and the results of two-dimensional, electrostatic particle simulations of this configuration, with emphasis on time-average transport.-- DOE Contract FG03-86ER53220, ONR Contract N00014-85-K-0809.

(1) P.L.Pritchett, F.V.Coroniti, J.Geophys.Res.,Vol.89, No.A1, p.168 (1984).

Bounded-Plasma Physics Workshop
University of California, Berkeley
September 22-23, 1986

Schedule of BPPW Presentations
Monday 22 September 1986

8:30 Registration and parking arrangements.
Coffee, tea, orange juice and rolls.

9:00 C.K. Birdsall(chairman). *Welcoming address and general information.*

C.K. Birdsall, (2)T.L. Crystal, P.C. Gray, S. Kuhn, and (1)Wm.S. Lawson
Introduction to **PDW1** *and Q-machine simulation; presentation of* "The Movie".

C.K. Birdsall, (1)T.L. Crystal, P.C. Gray, P. Krumm, (2)S. Kuhn, Wm.S. Lawson, M. Oertl, and N. Schupfer. *Trapped-electron effects on negative-bias d.c. states of a collisionless single-emitter plasma device: theory, simulation, and experiment.*

10:30 Coffee and posters of preceding talks.

11:15 K.S. Theilhaber. *Dynamics of the crossed-field sheath: a movie from the* **ES2** *code.*

S. Parker. *Electrostatic potentials due to nonuniform magnetic fields.*

D. Hewett (LLNL).
Electromagnetic boundary conditions for implicit codes.

12:15 Lunch in Kerr Campus dining hall Building 10 (the great hall). Posters.

K.S. Theilhaber(chairman).
1:30 (1)T.L. Crystal, M. Hörhager, (2)S. Kuhn, and (3)Wm.S. Lawson.
Theory and simulation of Pierce diode dynamics:
Linear and nonlinear features, plus nontrivial external circuit effects.

(1)C.K. Birdsall and P.C. Gray.
Small-amplitude impedance $Z(\omega)$ of a floating single-emitter plasma device.

2:30 Coffee and posters.

3:30 C.K. Birdsall, B.I. Cohen, and (1)R. Procassini.
Efficient incorporation of Coulomb collisions in bounded-plasma simulations.

L.A. Schwager. *Transport in the plasma sheath region near a wall.*

S. Kuhn. *Integral-equation approaches to bounded-plasma physics.*

5:00 Coffee and posters.

6:30 Dinner in executive dining room Building 10, Kerr Campus.

Authors listed alphabetically

(1),(2) means talks split

Schedule of BPPW Presentations
Tuesday 23 September 1986

8:30 Coffee, tea, orange juice and rolls.

T.L. Crystal(chairman).

9:00 (1) C.K. Birdsall and K.S. Theilhaber.
Source-sheath ion acceleration

P.C. Gray, (2)Wm.S. Lawson and (1)R.D. Pierce.
I -- V curves of the Child-Langmuir electron diode from particle simulations.

10:30 Coffee and posters of preceding talks.

(1)A. Wendt, M.A. Lieberman and H. Meuth.
Theory of nonuniform plasma in a planar magnetron discharge

(1) J. Helmer and K. Doniger.
Ion diagnostics in a planar magnetron discharge.

12:15 Lunch.

S. Kuhn(chairman).

1:30 T. Intrator (Wisconsin).
Some comments from experiments.

(1)Chris Goedde, M.A. Lieberman, A.J. Lichtenberg.
Stochastic electron heating in the sheaths of an RF discharge.

O. Buneman (Stanford).
Matching plasma radiation to free-space in spherical geometry using spherical harmonics (outward radiation only).

2:30 Coffee and posters.

3:30 O. Buneman (Stanford).
How to use a plasma boundary condition stated as $Z(\omega)$ in plasma simulation.

Panel discussion. M.A. Lieberman(chairman).
Concluding remarks from the steering committee... short! ... and open discussion.
Where are we, where do we want to go, and what should we do next?
⇒Should we have another BPPW in 1988?

SPECIAL SECTION V:

Plasma Theory & Simulation Research Group
Prof. C.K. Birdsall
EECS Department & Electronics Research Laboratory
University of California
Berkeley, CA 94720

Publications on
BOUNDED-PLASMA PHYSICS AND ENGINEERING

Our group began a transition into bounded plasma problems in 1981. Our new objective is to understand the dynamics of plasma sheaths at walls in terms of equilibrium, stability and transport. We also study other large potentials in plasmas, such as double layers and thermal barriers. The list here reflects the transition, a learning experience, starting with reports and talks, maturing into journal articles. Major support comes from DOE and ONR, plus help from Varian Associates-MICRO and Hughes.

1982

ERL Reports

C.K. Birdsall, "Plasma-Sheath-Wall Time-Dependent Behavior: An Informal Survey," Memo. No UCB/ERL M82/51, 22 June 1982, ERL, UC Berkeley. (58 pages). Talk at seminar lead by Dr. H. Ikegami at Biwa-ko, Japan, November 20,21, 1981.

Conference Proceedings

C.K. Birdsall, W.S. Lawson, A.B. Langdon, "Plasma-surface boundary conditions; plasma diodes," Proc. of Tenth Conf. on Numerical Simulation of Plasmas, San Diego, CA, Jan. 4-6, 1982.

C.K. Birdsall, "Sheath Formation and Fluctuations with Dynamic Electrons and Ions," presented at International Conference on Plasma Physics, June 9-15, 1982, Goteborg, Sweden; also appears in Conference proceedings.

C.K. Birdsall, "Electron Diode Dynamics; Limiting Currents; Plasma Diodes," presented at Symposium on Plasma Double Layers, Riso National Lab., Roskilde, Denmark; also appears in Symposium proceedings. June 16-18, 1982.

C.K. Birdsall, "Plasma Sheath Formation, Ion Acceleration, and Fluctuations in 'Steady' State," presented at IEEE International Conference on Plasma Science, Ottawa, Canada, May 17-19, 1982. Paper 1R7

Poster Papers/Talks

Division of Plasma Physics Annual Meeting, Nov. 1982, New Orleans:

C.K. Birdsall, "Temporal development of a plasma sheath; oscillatory vs. steady state," Bull. A.P.S. 27, page 1058, October 1982.

---

cf/updated July 1987; filename: bounded.pubs

1983

Journal Articles

K.Y. Kim, "Weak Monotonic Double Layers," *Physics Letters*, 97 A, 8 August 1983.

ERL Reports

Stephane Rousset, "Time-Dependent Child-Langmuir Diode Simulation," Memo. UCB/ERL M83/39, 11 July 1983.

K.Y. Kim, "Theory of Asymmetric Double Layers," Memo. UCB/ERL M83/45, 22 July 1983.

S. Kuhn, "Linear Longitudinal Oscillations in Collisionless Plasma Diodes With Thin Sheaths. Part I. Method", Memo. UCB/ERL M83/52, 31 August 1983.

S. Kuhn, "Linear Longitudinal Oscillations in Collisionless Plasma Diodes With Thin Sheaths. Part II. Application to an Extended Pierce-Type Problem," Memo. UCB.ERL M83/61, 3 October 1983.

Poster Papers/Talks

Tenth Conference on Numerical Simulation of Plasmas,January 4-6, 1983, San Diego, CA:

(1) C.K. Birdsall, W.S. Lawson, A.B. Langdon (LLNL), "Plasma-Surface Boundary Conditions;Plasma Diodes."

(2) W.S. Lawson, "A Technique for Non-Periodic Vlasov Grid Simulation."

APS/Division of Plasma in Physics, November 1983, Los Angeles, CA:

(1) S. Kuhn, "The General Perturbation Problem for the One-Dimensional Collisionless Plasma Diode."

(2) C.K. Birdsall, T.L. Crystal, S.Kuhn, A.B. Langdon, W.S. Lawson, N.F. Otani, "Plasma Diode Simulation: The PDW1 Code."

(3) Wm. S. Lawson, "Vlasov Simulation on a Finite Grid With A Discontinuous Distribution Function."

(4) N.Otani, "Scaling of Magnetized Double Layers."

(5) K.Y. Kim, "Weak Asymmetric Double Layers (ADL)."

(6) T.L. Crystal, S. Kuhn, Wm. Lawson, "Pierce Diode Instabilities and Extensions: Simulations With PDW1."

1984

Journal Articles

S.Kuhn, "Linear Longitudinal Oscillations in Collisionless Diodes with Thin Sheaths; Part I. Method," *Physics of Fluids* 27(7), 1821, July.

S.Kuhn, "Linear Longitudinal Oscillations in Collisionless Plasma Diodes with Thin Sheaths; Part II. Application to an Extended Pierce-type Problem," *Physics of Fluids*27(7), 1834, July.

ERL Reports

W.S. Lawson, "A Method for Simulation of Vlasov Systems with Discontinuous Distribution Functions and GASBAG User's Manual," Memo No. UCB/ERL M84/24, March, UC Berkeley.

W.S. Lawson, "PWD1 User's Manual," Memo No. UCB/ERL M84/37, April, UC Berkeley.

K.Y. Kim, "Vlasov-Poisson and Modified k-dV Theory and Simulation of Weak and Strong Double Layers," Memo No. UCB/ERL M84/47, June, UC Berkeley.

T.L. Crystal and S. Kuhn, "Particle simulation of the low-alpha Pierce diode," Memo No. UCB/ERL M84/74, 20 September 1984, UC Berkeley.

Poster Papers/Talks

International Conference on Plasma Physics, June 27-July 3, 1984, Lausanne, Switzerland:

(1) S. Kuhn, C.K. Birdsall, T.L. Crystal, P.L. Gray, William S. Lawson, "One dimensional particle simulations of the collisionless single-ended Q machine," (P8-11).

(2) T.L. Crystal and S. Kuhn, "Particle Simulations of the low-alpha Pierce diode," (P33-11).

Second Symposium on Plasma Double Layers and Related Topics, July 5-6, 1984, Innsbruck, Austria:

(1) P. Gray, S. Kuhn, T.L. Crystal and C.K. Birdsall, "Particle simulations of the unstable states of a collisionless single-end plasma device."

(2) N.F. Otani, "Evolution of ion holes and large potential structures in simulations of bounded current-driven magnetized plasma systems."

(3) K.Y. Kim and T.L. Crystal, "Theory and Simulation of Ion Acoustic Double Layers."

APS Division of Plasma Physics Meeting, November 1984, Boston, MA:

(1) C.K. Birdsall, William S. Lawson, T.L. Crystal, S. Kuhn, A.B. Langdon, "Plasma diode simulation: the PDW1 code."

(2) L.A. Schwager, "Simulation of charged particle reflection and emission effects in the plasma-sheath region."

IEEE Conference on Plasma Science, May 1984, St. Louis, MO:

(1) S. Kuhn, P.Gray, T.L. Crystal, C.K. Birdsall, "Axial Equilibria of Collisionless Single-Ended Q Machines: Particle Simulations versus Theory and Experiment." (10 minute movie)

(2) T.L. Crystal, S. Kuhn and C.K. Birdsall, "The Classical Pierce Diode: Using Particle Simulations on Linear and Nonlinear Behavior and Final States."

1985

Book

C.K. Birdsall, A.B. Langdon, *Plasma Physics via Computer Simulation*, McGraw-Hill, New York. See especially Chapters 14, 15, 16 on bounded plasmas.

Journal Articles

W.S. Lawson, "A Method for Simulation of Vlasov Systems with Discontinuous Distribution Functions," *J. of Computational Physics*, **61** (1), p. 51, October.

S. Ishiguro and T. Kamimura, "Double Layer Formation Caused by Contact Between Different Temperature Plasmas," *Physics of Fluids* **28** (7), pp. 2100-2105, July.

T.L. Crystal and S. Kuhn, "Particle Simulations of the Low-alpha Pierce Diode," *Physics of Fluids* **28** (7), pp. 2116-2124, July.

Reports

Bruce I. Cohen and Mark E. Stewart; Charles K. Birdsall, "Direct Implicit Particle Simulation of Tandem Mirrors," *LLNL Mirror Theory Monthly February 1985.*

C. K. Birdsall, T. L. Crystal, P. C. Gray and S. Kuhn, "Bounded Plasma Dynamics from Particle Simulations; Movie Script," Memo No. UCB/ERL M85/54, 2 July 1985, UC Berkeley.

Poster Papers/Talks

Sherwood Theory Conference, April 15-17, 1985, University of Wisconsin, Madison, Wisconsin:

L.A. Schwager and C.K. Birdsall, "A Model of the Plasma-Sheath Region Including Secondary Electron Emission and Ion Reflection."

Eleventh International Conference on Numerical Simulation of Plasma, Montreal, Quebec, Canada, 25-27 June 1985:

(1) C.K. Birdsall, W.S. Lawson, T. Crystal, S. Kuhn, N. Otani, I. Roth, and A.B. Langdon, "Problems of Bounded Particle Simulations and First Generation Solutions."

(2) B.I. Cohen, M.E. Stewart, and C.K. Birdsall, "Direct Implicit Particle Simulation of Tandem Mirror."

17th International Conference on Phenomena in Ionized Gases, Budapest, July 1985:

C.K. Birdsall, T.L. Crystal, P. Gray, and S. Kuhn, "Instability Of A Collisionless Single-Ended Plasma Device Operated In The Positive-Bias Electron-Rich Regime; From Simulations."

INTOR Specialists' Meeting On Impurity Control, IAEA Headquarters, Vienna, Austria:

C.K. Birdsall, "Boundary Conditions; Matching Plasma-Sheath-Wall." (invited paper)

APS/Division of Plasma Physics Annual Meeting, Nov 4-8, 1985, San Diego, CA:

(1) B.I. Cohen, M.E. Stewart, R.P. Freis (LLNL), L.A. Strugala, and C.K. Birdsall, "Direct Implicit Particle Simulation of Tandem Mirrors."

(2) Wm. Lawson, P.C. Gray, E.A. Adler, and C.K. Birdsall, "A Simulation Study of Effects of Emission Noise in a Thermionic Diode."

(3) P.C. Gray, T.L. Crystal, S. Kuhn, and C.K. Birdsall, " Equilibrium Corrections for Electron Hole Filling: Simulation vs. Theory."

(4) L.A. Schwager and C.K. Birdsall, "A Model of the Plasma-Sheath Region Including Secondary Electron Emission and Ion Reflection."

(5) A. Wendt, P.C. Gray, H. Meuth, M.A. Lieberman and C.K. Birdsall, "Experimental and Simulation Study of Planar Magnetron Discharges."

(6) C.K. Birdsall, P.C. Gray and T.L. Crystal, "A Simulation Study of the Dependence of the Plasma-Sheath Impedance on Frequency."

1986

Journal Articles

Charles K. Birdsall, Niels F. Otani and Bruce I. Cohen, "Simulation of Plasma Dynamics Using Many Particles," *IEEE Electrotechnology Review* **2**, pp. 43,44, 1986.

S. Kuhn and M. Hörhager, "External-circuit Effects on Pierce-Diode Stability Behavior," *J. Appl. Phys.* **60** (6), pp. 1952-1959, September 15, 1986.

Reports

William S. Lawson, "Linear Magnetized Plasma Response to an Oblique Electrostatic Wave," University of California, Berkeley, Memorandum No. UCB/ERL M86/94, December 15, 1986.

Poster Papers

APS Division of Plasma Physics Twenty-Eighth Annual Meeting, November 3-7, 1986, Baltimore, MD:

L.A. Schwager and C.K. Birdsall, "Transport across the Plasma-Wall Sheath with Secondary Electron Emission and Ion Reflection."

T.L. Crystal and S. Kuhn, " Pierce Diode Instability Simulations with External Inductance and Resistance."

S.E. Parker, C.K. Birdsall, and K. Theilhaber, "Electrostatic Effects on Confinement Outside the Separatrix of Field Reversed Configurations."

R.J. Procassini, C.K. Birdsall, and B.I. Cohen (LLNL), "Direct Implicit Particle Simulation of Tandem Mirrors."

K. Theilhaber and C.K. Birdsall, "Structure of the Crossed-Field Sheath." (with short movie)

Talks

C. K. Birdsall and the Plasma Theory and Simulation Group, "Planar Plasma Discharges: Simulations and Experiments," at Sandia National Labs, October 7, 1986.

C. K. Birdsall and Michael Lieberman, "Planar Plasma Discharges: Simulations and Experiments" at Varian Associates Technical Seminar, October 20, 1986.

Workshop

Bounded-Plasma Physics Workshop, University of California, Berkeley, September 22-23, 1986. See schedule following.

Bounded-Plasma Physics Workshop
University of California, Berkeley
September 22-23, 1986

Schedule of BPPW Presentations
Monday 22 September 1986

8:30 Registration and parking arrangements.
Coffee, tea, orange juice and rolls.

9:00 C.K. Birdsall(chairman). *Welcoming address and general information.*

C.K. Birdsall, (2)T.L. Crystal, P.C. Gray, S. Kuhn, and (1)Wm.S. Lawson
Introduction to **PDW1** *and Q-machine simulation; presentation of* "The Movie".

C.K. Birdsall, (1)T.L. Crystal, P.C. Gray, P. Krumm, (2)S. Kuhn, Wm.S. Lawson, M. Oertl, and N. Schupfer. *Trapped-electron effects on negative-bias d.c. states of a collisionless single-emitter plasma device: theory, simulation, and experiment.*

10:30 Coffee and posters of preceding talks.

11:15 K.S. Theilhaber. *Dynamics of the crossed-field sheath: a movie from the* **ES2** *code.*

S. Parker. *Electrostatic potentials due to nonuniform magnetic fields.*

D. Hewett (LLNL).
Electromagnetic boundary conditions for implicit codes.

12:15 Lunch in Kerr Campus dining hall Building 10 (the great hall). Posters.

K.S. Theilhaber(chairman).
1:30 (1)T.L. Crystal, M. Hörhager, (2)S. Kuhn, and (3)Wm.S. Lawson.
Theory and simulation of Pierce diode dynamics:
Linear and nonlinear features, plus nontrivial external circuit effects.

(1)C.K. Birdsall and P.C. Gray.
Small-amplitude impedance $Z(\omega)$ of a floating single-emitter plasma device.

2:30 Coffee and posters.

3:30 C.K. Birdsall, B.I. Cohen, and (1)R. Procassini.
Efficient incorporation of Coulomb collisions in bounded-plasma simulations.

L.A. Schwager. *Transport in the plasma sheath region near a wall.*

S. Kuhn. *Integral-equation approaches to bounded-plasma physics.*

5:00 Coffee and posters.

6:30 Dinner in executive dining room Building 10, Kerr Campus.

Authors listed alphabetically
(1),(2) means talks split

Schedule of BPPW Presentations
Tuesday 23 September 1986

8:30 Coffee, tea, orange juice and rolls.

T.L. Crystal(chairman).
9:00 (1) C.K. Birdsall and K.S. Theilhaber.
Source-sheath ion acceleration

P.C. Gray, (2)Wm.S. Lawson and (1)R.D. Pierce.
$I-V$ curves of the Child-Langmuir electron diode from particle simulations.

10:30 Coffee and posters of preceding talks.

(1)A. Wendt, M.A. Lieberman and H. Meuth.
Theory of nonuniform plasma in a planar magnetron discharge

(1) J. Helmer and K. Doniger.
Ion diagnostics in a planar magnetron discharge.

12:15 Lunch.

S. Kuhn(chairman).
1:30 T. Intrator (Wisconsin).
Some comments from experiments.

(1)Chris Goedde, M.A. Lieberman, A.J. Lichtenberg.
Stochastic electron heating in the sheaths of an RF discharge.

O. Buneman (Stanford).
Matching plasma radiation to free-space in spherical geometry using spherical harmonics (outward radiation only).

2:30 Coffee and posters.

3:30 O. Buneman (Stanford).
How to use a plasma boundary condition stated as $Z(\omega)$ in plasma simulation.

Panel discussion. M.A. Lieberman(chairman).
Concluding remarks from the steering committee... short! ... and open discussion.
Where are we, where do we want to go, and what should we do next?
⇒Should we have another BPPW in 1988?

Reports

William S. Lawson, "Computer Simulation of Bounded Plasma Systems," University of California, Berkeley, Memorandum No. UCB/ERL M87/14, March 5, 1987.

K. Theilhaber and C. K. Birdsall, "Vortex Dynamics and Transport to the Wall in a Crossed-Field Plasma Sheath," University of California, Berkeley, Memorandum No. UCB/ERL M87/18, April 10, 1987.

Kim Theilhaber, "ES2 User's Manual--Version 1," University of California, Berkeley, Memorandum No. UCB/ERL M87/23, May 11, 1987.

R. J. Procassini, C. K. Birdsall, E. C. Morse, and B. I. Cohen, "A Relativistic Monte Carlo Binary Collision Model for Use in Plasma Particle Simulation Codes," University of California, Berkeley, Memorandum No. UCB/ERL M87/24, May 14, 1987.

William S. Lawson, "Artificial Cooling Due to Quiet Injection in Bounded Plasma Particle Simulations," University of California, Berkeley, Memorandum No. UCB/ERL M87/34, May 21, 1987.

William S. Lawson, "The Pierce Diode with an External Circuit. I. Simulation in the Linear Regime," University of California, Berkeley, Memorandum No. UCB/ERL M87/51, July 1987.

William S. Lawson, "The Pierce Diode with an External Circuit. II. Non-uniform Equilibria," University of California, Berkeley, Memorandum No. UCB/ERL M87/52, July 1987.

William S. Lawson, "The Pierce Diode with an External Circuit. III. Chaotic Behavior," to be ERL Memo., 1987.

Lou Ann Schwager, "Effects of Secondary Electron Emission on the Collector and Source Sheaths Bounding a Finite Ion Temperature Plasma," to be ERL Memo., 1987.

Lou Ann Schwager, "Effects of Ion Reflection on the Collector and Source Sheaths Bounding a Finite Ion Temperature Plasma," to be ERL Memo., 1987.

Poster Papers/Talks

Poster Paper at U.S./Japan Seminar: Effects of Electric Fields on Magnetic Confinement, January 22-24, 1987, University of California, Los Angeles:

K. S. Theilhaber and C. K. Birdsall, "Large Electric Fields in a Magnetized Plasma Sheath: Long-lived Vortices."

Poster Papers at Sherwood Controlled Fusion Theory Conference, April 6-8, 1987, San Diego, California:

K. Theilhaber, "Transport Induced by a Crossed-Field Sheath."

Richard J. Procassini and Charles K. Birdsall, "Performance and Optimization of Direct Implicit Time Integration Schemes for Use in Electrostatic Particle Simulation Codes."

Lou Ann Schwager, "Collector Sheath and Source Sheath in a Collisionless Finite Ion Temperature Plasma with Secondary Electron Emission and Ion Reflection at the Bounding Surface."

Poster Papers at IEEE International Conference on Plasma Science, June 1-3, 1987, Arlington, Va.:

K. Theilhaber and C. K. Birdsall, "Large Electric Fields in a Magnetized Plasma Sheath; Long-lived Vortices."

L. A. Schwager and C. K. Birdsall, "Potential Drop and Transport in a Bounded Plasma Including Secondary Electron Emission and Ion Reflection at the Collector."

Invited talk at APS Division of Plasma Physics Twenty-Ninth Annual Meeting, November 2-6, 1987, San Diego, California:

K. Theilhaber, "Vortex Formation and Transport to the Wall in a Crossed-Field Sheath."

Poster Papers at APS Division of Plasma Physics Twenty-Ninth Annual Meeting, November 2-6, 1987, San Diego, California:

C. K. Birdsall, K. S. Theilhaber, and S. Kuhn, "Ion Acceleration in a Plasma Source Sheath."

A. Friedman and S. L. Ray, *LLNL*, and S. Parker and C. K. Birdsall, *U. C. Berkeley*, "Prospects for Multi-Scale Particle-in-Cell Simulation of Plasmas."

Wm. S. Lawson, "Investigations of the Pierce Diode Strange Attractor."

S. E. Parker and C.K. Birdsall, *U. C. Berkeley*, and A. Friedman and S. L. Ray, *LLNL*, "Direct Implicit Particle Simulation of a Bounded Plasma System."

R. J. Procassini, J. C. Cummings and C. K. Birdsall, *University of California, Berkeley*, and B. I. Cohen, *Lawrence Livermore National Laboratory*, "Direct Implicit Particle Simulation of Simple Mirrors."

L. A. Schwager, "The Effect of Thermionic and Secondary Electron Emission at the Collector on Potential Drop and Transport Through the Plasma-Sheath Region."

DISTRIBUTION LIST

AFWL/DYP
Pettus

Department of Energy
Hitchcock, Katz, Lankford, Macrusky, Manley, Nelson, Sadowski, Tech. Info. Center

Department of Navy
Condell, Florance, Roberson

Argonne National Laboratory
Brooks

Austin Research Associates
Drummond, Moore

Bell Telephone Laboratories
Hasegawa

Berkeley Research Assoc.
Brecht, Orens, Thomas

Berkeley Scholars, In.
Ambrosiano

Cal. Inst. of Technology
Bridges, Gould

Calif. State Polytech. Univ.
Rathmann

Cambridge Research Labs.
Rubin

Columbia University
Chu

Dartmouth
Hudson, Lotko

E. P. R. I.
Scott

GA Technologies
Bernard, Evans, Helton, Lee

GTE Laboratories
Rogoff, Winsor

Hascomb Air Force Base
Rubin

Hewlett-Packard Laboratories
Gleason, Marcoux

Hughes Aircraft Co., Torrance
Adler, Longo

Hughes Research Lab., Malibu
Harvey, Hyman, Poeschel, Schumacker

Institute of Fusion Studies, Texas
Librarian

JAYCOR
Klein, Tumolillo

JPL
Liewer

Kaman Science Corp.
Hobbs

Lawrence Berkeley Laboratory
Cooper, Kaufman, Kunkel.

Lawrence Livermore National Lab.
Albritton, Anderson, Barr, Brengle, Briggs, Bruijnes, Byers, Chambers, Chen, B.Cohen, R. Cohen, Denavit, Estabrook, Fawley, Fowler, Friedman, Freis, Fuss, Harte, Hewett, Killeen, Kruer, Langdon, Lasinski, Lee, Maron, Matsuda, Max, Nevins, Nielsen, Smith, Tull, Ziolkowski

Lockheed
Siambis

Los Alamos Scientific Lab.
Barnes, Borovsky, Forslund, Kwan, Lindemuth, Mason, Nielson, Oliphant, Peratt, Sgro, Thode

Mass. Inst. of Technology
Berman, Bers, Gerver, Lane, Palevsky

Mission Research Corporation
Godfrey, Mostrom

Naval Research Laboratory
Boris, Craig, Haber, Joyce, Orens, Roberson, Vomvoridis

New York University
Grad, Otani, Weitzner

Northeastern University
Chan, Silevitch

Oak Ridge National Lab.
Fusion Energy Library, Lebouef, Meier, Mook

Filename: qpr.distrlist

Physics International
Woo

Princeton Plasma Physics Lab
Chen, Cheng, Lee, Okuda, Tang, Graydon, Librarian

SAIC - Boulder
D'Ippolito, Myra

SAIC - Virginia
Drobot, Mankofsky, McBride, Smith

Sandia Labs, Albuquerque
Freeman, Humphries, Poukey, Quintenz, Wright

Sandia Labs, Livermore
Marx, Wilson, Hsu

Stanford University
Blake, Buneman, Gledhill Physics Library, Storey

TRW
Wagner

University of Arizona
Carlile

University of California, Berkeley
Arons, Birdsall, Chorin, Cook, Crystal, Graves, Haller, Hess, Lawson, Lichtenberg, Lieberman, McKee, Morse, Parker, Pierce, Procassini, Roth, Schwager, Theilhaber

University of California, Davis
DeGroot

University of California, Irvine
Rynn

University of California, Los Angeles
Abdou, Dawson, Decyk, Prinja

University of Illinois
Kushner

University of Iowa
Joyce, Knorr, Nicholson

University of Maryland
Guillory, Rowland, Winske

University of New Mexico
Anderson, Humphries

University of Pittsburgh
Zabusky

University of Southern California
Kuehl

University of Texas
Horton, McMahon, Tajima

University of Washington
Potter

University of Wisconsin
Emmert, Hershkovitz, Intrator, Shohet

Varian Associates
Anderson, Helmer

Universität Innsbruck
Cap, Kuhn

I.N.P.E.
Bittencourt, Montes

University of Toronto
Stangeby

Riso National Laboratories
Lynov, Pecseli

Culham Laboratory
Eastwood

Imperial College
Burger

Oxford University
Allen, Benjamin, Edgley

University of Reading
Hockney

Ecole Polytechnique, Palaiseau
Adam

Universite Paris
Raviart

IPP-KFA
Reiter

Max Planck Institute für Plasmaphysik
Biskamp, Chodura

University Bayreuth
Schamel

Universität Kaiserslautern
Wick

Israel
Gell

Tel Aviv University
Cuperman

Hiroshima University
Tanaka

Kyoto University
Abe, Matsumoto, Jimbo

Nagoya University
Kamimura, Research Info. Center

Osaka University
Mima, Nishihara

Shizuoka University
Saeki

Tohoku University
Sato

University of Tromso
Armstrong, Trulsen

Centro de Electrodinàmica, Lisbon
Brinca

Ecole Polytechnique, Lausanne
Hollenstein

END

DATE

FILMED

JAN

1988